

## Novel *N*-Acetyl Bioisosteres of Melatonin: Melatonergic Receptor Pharmacology, Physicochemical Studies, and Phenotypic Assessment of their Neurogenic Potential

Mario de la Fuente Revenga, Nerea Fernández-Sáez, Clara Herrera-Arozamena, José A. Morales-García, Sandra Alonso-Gil, Ana Pérez-Castillo, Daniel Henri Caignard, Silvia Rivara, and María Isabel Rodríguez-Franco

*J. Med. Chem.*, **Just Accepted Manuscript** • DOI: 10.1021/acs.jmedchem.5b00245 • Publication Date (Web): 29 May 2015

Downloaded from <http://pubs.acs.org> on June 10, 2015

### Just Accepted

"Just Accepted" manuscripts have been peer-reviewed and accepted for publication. They are posted online prior to technical editing, formatting for publication and author proofing. The American Chemical Society provides "Just Accepted" as a free service to the research community to expedite the dissemination of scientific material as soon as possible after acceptance. "Just Accepted" manuscripts appear in full in PDF format accompanied by an HTML abstract. "Just Accepted" manuscripts have been fully peer reviewed, but should not be considered the official version of record. They are accessible to all readers and citable by the Digital Object Identifier (DOI®). "Just Accepted" is an optional service offered to authors. Therefore, the "Just Accepted" Web site may not include all articles that will be published in the journal. After a manuscript is technically edited and formatted, it will be removed from the "Just Accepted" Web site and published as an ASAP article. Note that technical editing may introduce minor changes to the manuscript text and/or graphics which could affect content, and all legal disclaimers and ethical guidelines that apply to the journal pertain. ACS cannot be held responsible for errors or consequences arising from the use of information contained in these "Just Accepted" manuscripts.



**ACS Publications**  
High quality. High impact.

**Novel *N*-Acetyl Bioisosteres of Melatonin: Melatonergic  
Receptor Pharmacology, Physicochemical Studies, and  
Phenotypic Assessment of their Neurogenic Potential**

Mario de la Fuente Revenga,<sup>†</sup> Nerea Fernández-Sáez,<sup>†</sup> Clara Herrera-Arozamena,<sup>†</sup>  
José A. Morales-García,<sup>‡,§</sup> Sandra Alonso-Gil,<sup>‡,§</sup> Ana Pérez-Castillo,<sup>‡,§</sup> Daniel-Henri  
Caignard,<sup>#</sup> Silvia Rivara,<sup>⊥</sup> and María Isabel Rodríguez-Franco<sup>\*,†</sup>

<sup>†</sup>Instituto de Química Médica, Consejo Superior de Investigaciones Científicas (IQM-CSIC), C/ Juan de la Cierva 3, 28006-Madrid, Spain.

<sup>‡</sup>Instituto de Investigaciones Biomédicas “Alberto Sols”, Consejo Superior de Investigaciones Científicas (IIB-CSIC), C/Arturo Duperier 4, 28029-Madrid, Spain.

<sup>§</sup>Centro de Investigación Biomédica en Red sobre Enfermedades Neurodegenerativas (CIBERNED), C/ Valderrebollo 5, 28031-Madrid, Spain.

<sup>#</sup>Institut de Recherches Servier, 125 Chemin de Ronde, 78290-Croissy sur Seine, France.

<sup>⊥</sup>Dipartimento di Farmacia, Università degli Studi di Parma, Parco Area delle Scienze 27/A, 43124-Parma (Italy).

*Dedicated to our dear colleague Prof. José Elguero on the occasion of his 80<sup>th</sup> birthday*

**ABSTRACT**

Herein we present a new family of melatonin-based compounds, in which the acetamido group of melatonin has been bioisosterically replaced by a series of reversed amides and azoles, such as oxazole, 1,2,4-oxadiazole and 1,3,4-oxadiazole, as well as other related 5-membered heterocycles, namely 1,3,4-oxadiazol-(thio)ones, 1,3,4-triazol-(thio)ones and an 1,3,4-aminothiadiazole. New compounds were fully characterized at melatonin receptors (MT<sub>1</sub>R and MT<sub>2</sub>R), and results were rationalized by superimposition studies of their structures to the bioactive conformation of melatonin. We also found that several of these melatonin-based compounds promoted differentiation of rat neural stem cells to a neuronal phenotype *in vitro*, in some cases to a higher extent than melatonin. This unique profile constitutes the starting point for further pharmacological studies to assess the mechanistic pathways, and the relevance of neurogenesis induced by melatonin-related structures.

## INTRODUCTION

Melatonin (Figure 1) is a neurohormone produced in different tissues, primarily in the pineal gland, but also in retina and gastrointestinal tract. Beyond its fundamental role in circadian and seasonal rhythms' regulation, melatonin is involved in a variety of physiological processes like the modulation of immune and endogenous antioxidant systems, among others.<sup>1</sup> Due to this wide array of biologically-relevant activities, research efforts aiming to identify new melatonergic analogues increase continuously.<sup>2</sup>

Two G-protein-coupled receptors (GPCRs), named MT<sub>1</sub> and MT<sub>2</sub> (MT<sub>1</sub>R and MT<sub>2</sub>R), mediate most of the melatonin physiological and pharmacological actions. These melatonin receptors (MTRs) lack a crystalized structure that could allow the characterization of their tertiary structure and the pattern of interactions undertaken with their ligands. A number of homology models of the MT<sub>1</sub>R and MT<sub>2</sub>R have been built, although the low identity of their sequences with the used templates increases the speculation degree, thus limiting the utility of these models for drug design purposes.<sup>2,3</sup> In this regard, ligand-based design of novel melatonergic agents is still widely exploited. This approach has provided three approved melatonergic ligands, besides melatonin itself: agomelatine for major depression, ramelteon for sleep disorders and tasimelteon for non-24-hour sleep-wake disorder (Figure 1), whilst others are in developmental stages.<sup>4</sup>

Subtle and major changes in the structure of melatonin have led to a plethora of ligands, in many cases able to surpass the picomolar affinity of the endogenous agonist. Based on these studies, several pharmacophoric models have been proposed.<sup>5-7</sup> Among these pharmacophores, there is a wide consensus about the necessity of an oxygen atom attached to the aromatic or heteroaromatic core connected to the acetamido-containing side chain. Deletion of the methoxy group generally provokes a decrease in intrinsic

activity, like is the case of the antagonist luzindole (Figure 1). Regarding the indole nucleus, there are numerous examples of aromatic scaffold hopping, like agomelatine and other naphthalenic derivatives, which demonstrate that the presence of the indole-NH is not essential for activity.<sup>8-10</sup> Exploitation of a putative lipophilic pocket close to the binding site of melatonin has led to the development of nonselective and MT<sub>2</sub>R-selective ligands,<sup>11</sup> and has yielded key pharmacological tools, like luzindole or the radioligand 2-[<sup>125</sup>I]iodomelatonin.<sup>12-14</sup> Both indole replacement and utilization of the abovementioned non-polar cavity had proven to be successful approaches, although usually resulted in an overall increase of the lipophilicity that generally undermines drug-like properties.<sup>15-17</sup> Therefore, from a drug discovery point of view, it is more desirable to increase the enthalpic component of the binding free-energy (e.g., hydrogen bonds, multipolar and cation- $\pi$  interactions) via optimization of specific polar interactions.<sup>18</sup>

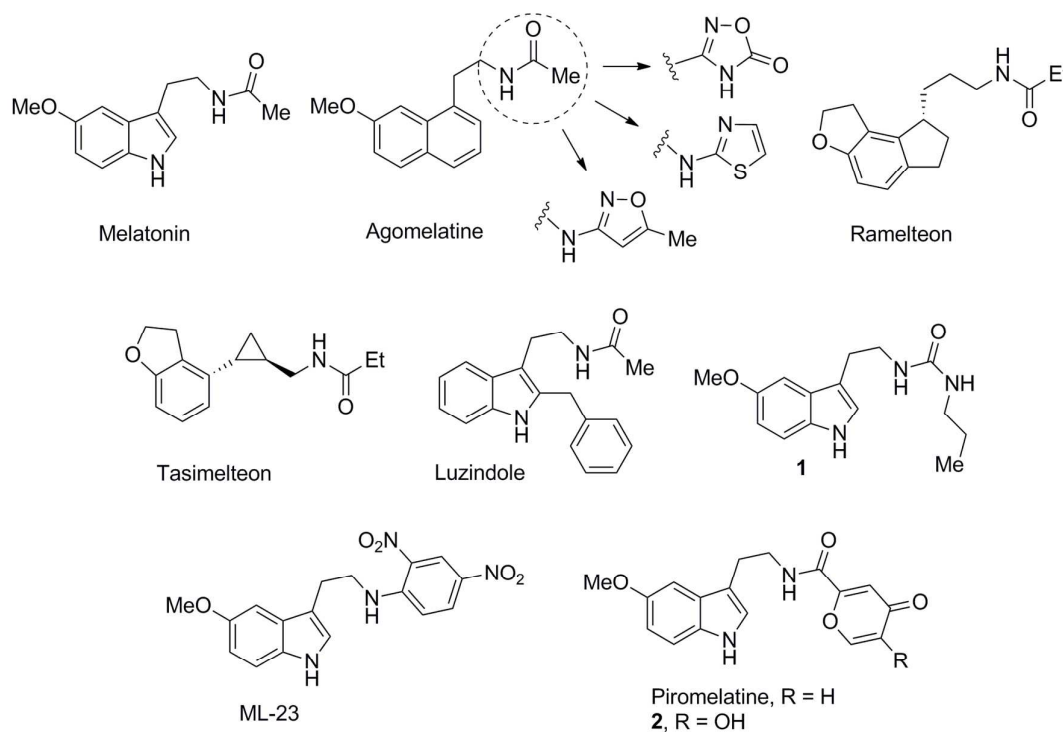


**Figure 1.** Melatonergic drugs on the market and other selected melatonergic ligands.

Reported modifications on the acetamido group of melatonin were discouraging, as generally resulted in a significant decrease, or total loss, of binding affinity and potency at MT<sub>1</sub>R and MT<sub>2</sub>R. Indeed, there are few described cases of bioisosterism in which the acetamido group has been replaced by other carbamoyl moieties whilst the 5-methoxytryptamine skeleton was kept intact, such as the propyl urea **1**<sup>19</sup> and *N*-(2-(5-methoxy-1*H*-indol-3-yl)ethyl)-2,4-dinitroaniline (ML-23).<sup>20,21</sup> Piromelatine and its hydroxyl analogue **2** represent examples of atypical acylation of the tryptamine core with a 4*H*-pyran-4-one fragment, able to retain significantly good affinities.<sup>22-24</sup> More recently, Rami et al. described the use of 5-membered heterocycles replacing for either the acyl or the whole acetamido group over the structure of agomelatine, generally maintaining good binding affinities for MTRs.<sup>25</sup>

The acetamido group of melatonin has been proposed to intervene in captodative hydrogen bonds.<sup>3</sup> Therefore, its bioisosteric replacement could represent a useful strategy for the structural understanding of the not so well-known properties of the binding pocket of this fragment, in terms of size, shape, electronic distribution and lipophilicity. Exploitation of specific polar interactions occurring in this pocket with acetamido-like moieties may result in a greater enthalpy-driven binding of ligands. Herein, we have replaced the *N*-acetyl fragment of melatonin with a series of reversed unsaturated amides and some well-established amide bioisosteres: oxazole, 1,2,4-oxadiazole and 1,3,4-oxadiazole;<sup>26</sup> as well as other related acidic azoles bearing a hydrogen that could intervene in hydrogen bonds: 1,3,4-oxadiazol-(thio)ones, 1,3,4-triazol-(thio)ones and 1,3,4-aminothiazole (Figure 2). On another hand, the naturally occurring alkaloid 5-methoxy-*N,N*-dimethyltryptamine (5-MeO-DMT) that shows high affinity for several serotonin receptor populations,<sup>27</sup> is also known to displace 2-[<sup>125</sup>I]iodomelatonin from hamster brain membranes.<sup>28</sup> This indoleamine was included in

the study to investigate the ability of its dimethylamino substituent to bind human MTRs. The thermodynamic solubility at pH 7.4 of representative compounds of each family showing significant binding to MTRs was determined. Considering the high degree of similarity in the series, their relative hydrophilic nature was inferred from solubility values. For those azole compounds capable of undergoing an acid-base equilibrium, the solubility was also determined at different pH values in order to study their acid or basic character.<sup>29</sup>

Beyond ligand-MTRs interactions, we also put our focus on one outstanding property among the pleiotropic actions of melatonin: its ability to promote neurogenesis in the adult brain.<sup>30</sup> Neurogenesis involves the generation, maturation and integration of new neurons in the neuron circuitry, which is a widespread phenomenon during embryonic development. In the adult brain, neurogenesis remains vestigial and only two areas retain a significant continuous neurogenic turnover, namely the subventricular zone (SVZ) and the subgranular zone (SGZ) in the dentate gyrus of the hippocampus.<sup>31</sup> Neurogenesis appears to modulate learning and memory integration processes<sup>32</sup> and is sensitive to physiological, pathological and pharmacological stimuli.<sup>33</sup> For instance, ageing, neurodegenerative, and some mental diseases are associated with an exponential decrease in hippocampal neurogenesis.<sup>34</sup> Therefore, the controlled pharmacological stimulation of the endogenous neural stem cells from adult brain neurogenic niches might counteract the age-related loss of memory and cognitive deterioration in some pathological processes.<sup>35</sup>

Melatonin plasma levels decline along with age in a similar manner as the neurogenic rate does.<sup>36</sup> Whether the two phenomena are related or not, remains unclear, albeit melatonin positively modulates hippocampal neurogenesis by increasing both precursor cell proliferation and survival, and delays the decline of neurogenesis in the

hippocampi of aged mice.<sup>37,38</sup> This behaviour is in agreement with previous observations showing that exogenous melatonin administration, in addition to a much better retained cognitive performance, ameliorates the process of ageing by delaying the onset of deteriorated health stages in senescent mice.<sup>39</sup> Given the abovementioned properties of melatonin<sup>37</sup> and our interest in developing new melatonin-based compounds<sup>40-42</sup> with potential brain-repairing actions,<sup>43,44</sup> we conducted a phenotypic screening *in vitro* to assess the neurogenic potential of new derivatives using rat neural stem cells.

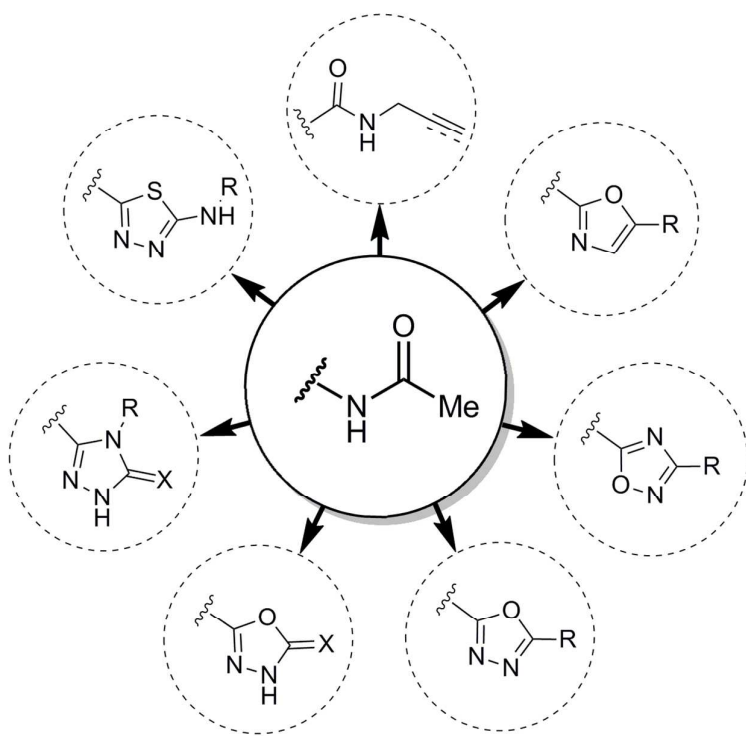


**Figure 2.** Illustration showing the replacement of the acetamido moiety of melatonin carried out in this work.



## RESULTS

**Synthesis of New Melatonin-Based Compounds.** The synthesis of all compounds here described is depicted in Scheme 1.

*Synthesis of retroamides and oxazoles.* *N*-Propargyl- and *N*-allyl-indolylamides **3-6** were obtained in good yields from commercial 2-(5-methoxy-1*H*-indol-3-yl)alkanoic acids that were activated with carbonyldiimidazole (CDI) and then treated with propargylamine or allylamine. Subsequently, propargyl amides **3** and **4** underwent a gold(III)-catalysed cycloisomerization,<sup>45,46</sup> affording the corresponding oxazoles **7** and **8** in moderate yields.

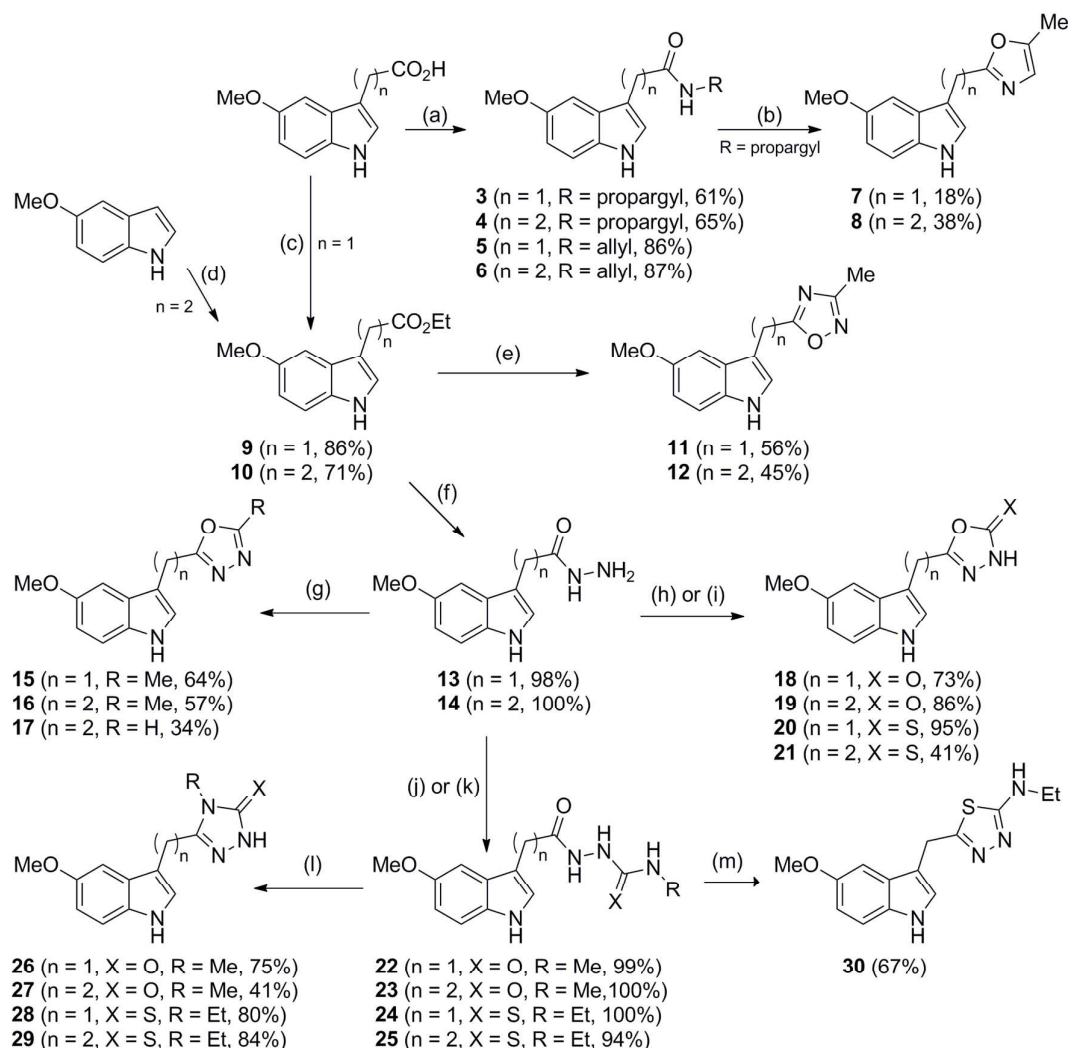
*Synthesis of 1,2,4- and 1,3,4-oxadiazoles.* Intermediate ester **9** was synthesised by acid-catalysed esterification from 2-(5-methoxy-1*H*-indol-3-yl)acetic acid. Ester **10** was obtained in good yield via Michael addition of the electron-rich 5-methoxyindole with ethyl acrylate catalysed by anhydrous zirconium (IV) chloride.<sup>47</sup> 1,2,4-Oxadiazoles **11** and **12** were prepared directly from the corresponding esters **9** and **10** by cyclocondensation with acetamidoxime in fair yields.<sup>48</sup> To obtain 1,3,4-oxadiazole isomers, esters **9** and **10** were subjected to a microwave-promoted hydrazinolysis giving intermediate hydrazides **13** and **14** in quantitative yields. Then, these hydrazides underwent a condensation with the corresponding orthoester in acidic medium to afford 1,3,4-oxadiazoles **15-17**, in moderate to fair yields.

*Synthesis of 1,3,4-oxadiazol-2-(thio)ones.* The microwave-heating of hydrazides **13** and **14** with CDI and triethylamine (TEA) afforded the corresponding 1,3,4-oxadiazol-2-ones **18** and **19**. Similarly, the use of carbon disulfide in basic medium afforded 1,3,4-oxadiazol-2-thiones **20** and **21**.

*Synthesis of 4-alkyl-1,2,4-triazol-5-(thio)ones and 2-amino-1,3,4-thiadiazole.* Reaction of hydrazides **13** and **14** with methylisocyanate or ethylisothiocyanate afforded

the corresponding acylsemicarbazides **22** and **23**, or acylthiosemicarbazides **24** and **25**, which underwent microwave-induced cyclocondensation in basic medium to give 4-methyl-1,2,4-triazol-5-ones **26** and **27**, and 4-ethyl-1,2,4-triazol-5-thiones **28** and **29** in good and very good yields, respectively. There are several methods in the literature for the synthesis of 2-amino-1,3,4-oxadiazoles and 2-amino-1,3,4-thiadiazoles from acylsemicarbazides and acylthiosemicarbazides. After some failed attempts with sulfuric acid<sup>49</sup> and P<sup>v</sup>-reagent,<sup>26</sup> only in the case of acylthiosemicarbazide **24** successful cyclization to 2-amino-1,3,4-thiadiazole **30** was achieved with phosphorus oxychloride at room temperature in fair yield.

All new melatonin-based derivatives were purified by chromatographic techniques and structurally characterized by their analytical and spectroscopic data (HPLC, <sup>1</sup>H NMR, <sup>13</sup>C NMR and HRMS). Compounds **18-21**, **26-30** can exist in two possible tautomers; for each compound, the major species (which is depicted in Scheme 1) was determined by a combination of NMR bidimensional experiments, such as COSY (homonuclear correlation spectroscopy), HSQC (heteronuclear single quantum coherence) and HMBC (heteronuclear multiple bond correlation) diagrams (see Supporting Information for further details).



**Scheme 1.** *Reagents and conditions:* (a) CDI, CH<sub>2</sub>Cl<sub>2</sub>, propargylamine or allylamine, rt; (b) AuCl<sub>3</sub>, CH<sub>2</sub>Cl<sub>2</sub>, N<sub>2</sub>, rt; (c) H<sub>2</sub>SO<sub>4</sub> (cat.), EtOH, reflux; (d) ethylacrylate, ZrCl<sub>4</sub> (anh.), CH<sub>2</sub>Cl<sub>2</sub>, N<sub>2</sub>, rt; (e) acetamidoxime, NaH, THF, mol. sieves, 80 °C; (f) hydrazine hydrate, 150 °C (mw), 45 min; (g) orthoester, AcOH (cat.), 125 °C (mw), 1 h; (h) compounds with X = O: CDI, TEA, THF, 100 °C (mw), 10 min; (i) compounds with X = S: CS<sub>2</sub>, EtOH, KOH (aq.), 150 °C (mw), 10 min; (j) intermediates with X = O and R = Me: MeNCO, EtOH, rt; (k) intermediates with X = S and R = Et: EtSCN, EtOH, rt; (l) NaOH (aq.), EtOH, 100 °C (mw), 15 min; (m) POCl<sub>3</sub>, rt.

**Pharmacology. Characterization at human MT<sub>1</sub>R and MT<sub>2</sub>R.** Binding and functional activity studies of new compounds were carried out at human MT<sub>1</sub>R or MT<sub>2</sub>R stably transfected in Chinese hamster ovary cells (CHO), using 2-[<sup>125</sup>I]iodomelatonin as radioligand and following described protocols.<sup>50</sup> The binding affinities are gathered in Table 1. Retroamides with unsaturated side chains (**3-6**) showed the highest affinities, with *K<sub>i</sub>*s in the low nano- and sub-nanomolar range. The alkenyl or alkynyl substitution does not significantly affect the potency of compounds. Conversely, the length of the spacer does; ethylene spacer is preferred in both cases (**4** and **6**). Compound **6** showed the highest affinities towards MTRs of all the series, displaying only 3-fold lower value than melatonin at MT<sub>2</sub>R.

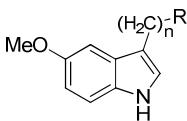
Binding affinities of oxadiazole-bearing compounds are more favoured by the presence of a methylene (**11** and **15**) than an ethylene spacer (**12**, **16**). Compared to **16**, absence of the methyl substituent in the 1,3,4-oxadiazole **17** slightly increased affinity. The heteroaromatic isomerism, that is 1,2,4- and 1,3,4-oxadiazole, does not seem relevant in the case of methylene-oxadiazoles (**11**, **15**). Conversely, in the case of ethylene-counterparts, the 1,3,4-oxadiazole (**16**) showed higher affinity than the 1,2,4-oxadiazole (**12**). 1,3-Oxazoles **7** and **8** show lower binding affinities than oxadiazole derivatives.

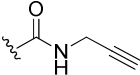
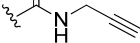
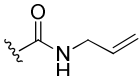
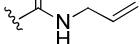
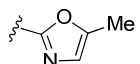
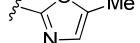
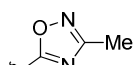
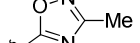
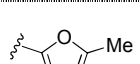
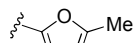
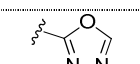
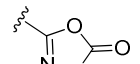
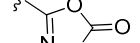
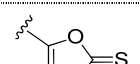
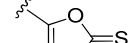
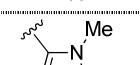
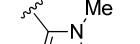
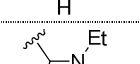
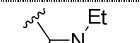
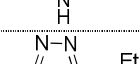
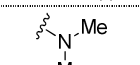
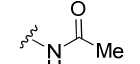
1,3,4-Oxadiazolones and -thiones (**18-21**), together with 1,3,4-triazol-ones and -thiones (**26-29**) display a dramatic drop in binding affinity, with the remarkable exception of 1,3,4-oxadiazolone **19**, which was the compound with the highest affinity for both MT<sub>1</sub>R (*K<sub>i</sub>* = 35 nM) and MT<sub>2</sub>R (*K<sub>i</sub>* = 4 nM) of all synthesized azole derivatives.

The compound with the most marked selectivity profile [*K<sub>i</sub>* (MT<sub>1</sub>) / (*K<sub>i</sub>* MT<sub>2</sub>) > 500], together with rather good binding affinity at the MT<sub>2</sub> subtype (*K<sub>i</sub>* = 17 nM) is the 2-amino-1,3,4-thiadiazole derivative **30**. Unfortunately, the synthesis of other amino-

azoles was not accomplished. Compared to **30**, the dimethylamino derivative 5-MeO-DMT is equipotent at MT<sub>2</sub>R ( $K_i = 16$  nM), but shows much milder selectivity (around 10-fold).

**Table 1.** Radioligand displacement binding studies at human MT<sub>1</sub>R and MT<sub>2</sub>R (*K<sub>i</sub>* ± SEM, nM).



Compd.	n	R	MT <sub>1</sub> R	MT <sub>2</sub> R	Ratio (MT <sub>1</sub> /MT <sub>2</sub> ) <sup>a</sup>
3	1		14 ± 4	3.8 ± 0.5	3.6
4	2		5.0 ± 0.9	1.0 ± 0.6	5
5	1		17 ± 0.7	4.9 ± 0.4	3.5
6	2		2.5 ± 0.2	0.45 ± 0.08	5.5
7	1		280 ± 20	>1000	-
8	2		>1000	498 ± 11	-
11	1		170 ± 15	44 ± 3	3.9
12	2		>1000	>1000	-
15	1		210 ± 10	16 ± 3	10
16	2		709 ± 10	190 ± 8	3.6
17	2		570 ± 10	68 ± 15	8.6
18	1		>1000	160 ± 50	-
19	2		35 ± 1	4 ± 0.5	10
20	1		>1000	535 ± 30	-
21	2		>1000	530 ± 50	-
26	1		>1000	560 ± 60	-
27	2		>1000	>1000	-
28	1		>1000	220 ± 50	-
29	2		>1000	>1000	-
30	1		>1000	17 ± 3	>500
5-MeO-DMT	2		210 ± 10	16 ± 0.5	10
Melatonin	2		0.091 ± 0.005	0.15 ± 0.07	0.6

<sup>a</sup>Ratio calculated only for compounds with *K<sub>i</sub>* < 100 nM for either of the subtypes.

1  
2  
3 Only compounds showing significant affinity for either receptor ( $K_i < 1000$  nM)  
4  
5 were functionally characterized in the [ $^{35}$ S]GTP $\gamma$ S binding assay, and results are  
6  
7 summarized in Table 2. The most potent compounds were retroamides, where the spacer  
8  
9 length determined the intrinsic activity and potency in each pair of derivatives.  
10  
11 Compounds **3** and **5** with a methylene linker were partial agonists, whereas those  
12  
13 bearing an ethylene, **4** and **6**, were full agonists. Azole-containing compounds showed a  
14  
15 very similar profile, weak partial agonism at MT<sub>2</sub>R and little or no effect at MT<sub>1</sub>R. Only  
16  
17 compounds **15** and **19** displayed EC<sub>50</sub> values in the 10<sup>-8</sup> M range at MT<sub>2</sub>R. 5-MeO-  
18  
19 DMT was nearly equipotent at both receptor subtypes but showed higher efficacy at the  
20  
21 MT<sub>1</sub>R than at the MT<sub>2</sub>R.  
22  
23  
24  
25  
26  
27  
28  
29  
30  
31  
32  
33  
34  
35  
36  
37  
38  
39  
40  
41  
42  
43  
44  
45  
46  
47  
48  
49  
50  
51  
52  
53  
54  
55  
56  
57  
58  
59  
60

Table 2. Functional studies (GTPγS) at MT<sub>1</sub>R and MT<sub>2</sub>R of selected compounds

MeO

(H<sub>2</sub>C)<sup>n</sup><sub>n</sub>

R

H

Compd.	n	R	MT <sub>1</sub> R		MT <sub>2</sub> R	
			EC <sub>50</sub> (nM)	E <sub>max</sub> (%)	EC <sub>50</sub> (nM)	E <sub>max</sub> (%) <sup>a</sup>
3	1		289 ± 13	67 ± 8	81 ± 3	82 ± 5
4	2		38 ± 3	106 ± 9	3 ± 0.3	99 ± 9
5	1		525 ± 31	64 ± 4	132 ± 70	70 ± 8
6	2		204 ± 54	92 ± 2	11 ± 9	88 ± 4
7	1		989 ± 23	23 ± 4	nd	nd
8	2		nd	nd	503 ± 5	32 ± 1
11	1		711 ± 23	16 ± 2	295 ± 13	48 ± 2
15	1		>1000	nd	71 ± 28	24 ± 3
16	2		961 ± 16	19 ± 6	881 ± 23	32 ± 4
17	2		>1000	nd	457 ± 141	25 ± 2
18	1		nd	nd	>1000	nd
19	2		326 ± 30	26 ± 4	29 ± 3	30 ± 3
20	1		nd	nd	>1000	nd
21	2		nd	nd	1096 ± 316	32 ± 9
26	1		nd	nd	>1000	nd
28	1		nd	nd	>1000	nd
30	1		nd	nd	110 ± 25	35 ± 7
5-MeO-DMT	2		257 ± 98	62 ± 3	112 ± 110	28 ± 3
Melatonin	2		0.098 ± 0.003	100	0.069 ± 0.003	100

nd: not determined. <sup>a</sup>Full agonist: E<sub>max</sub> > 80%; Partial agonist: 20% < E<sub>max</sub> < 80%; Antagonist: E<sub>max</sub> < 20%.<sup>50</sup>



**Thermodynamic solubility studies.** The thermodynamic solubility of a selection of azoles was determined in buffer at pH 7.4 (Table 3), following described protocols.<sup>51,52</sup> For comparison purposes, agomelatine and melatonin were also included. Melatonin was the most soluble compound at physiologic pH. No significant differences were found between 1,2,3-oxadiazole **11** and 1,3,4-oxadiazole **15** at pH 7.4; both compounds showed a solubility similar to that of agomelatine. Additionally, for those compounds bearing acidic or basic azoles, solubility was also determined at pH 5.5 and pH 9.3 as an indirect estimation of their acid-base properties. The solubility of **19**, **21**, **27**, and **29** showed a clear dependence on the pH, peaking at basic pH values. It is especially notable in the case of **19** and **21**, demonstrating the acidic nature of these compounds. The presence of the thione group in **21**, compared to the ketone in **19**, increases the pH dependence in solubility. 2-Amino-1,3,4-thiadiazole derivative **30** also showed a mild pH difference of its solubility, higher at acidic pH, according to a weak basic nature.<sup>53</sup>

**Table 3.** Thermodynamic solubility ( $\mu\text{M}$ ) of selected compounds.<sup>a</sup>

Compd.	pH 5.5	pH 7.4	pH 9.3
Melatonin	nd	6640 $\pm$ 25	nd
Agomelatine	nd	804 $\pm$ 24	nd
<b>11</b>	nd	1165 $\pm$ 23	nd
<b>15</b>	nd	970 $\pm$ 8	nd
<b>19</b>	1406 $\pm$ 1	2100 $\pm$ 20	7920 $\pm$ 30
<b>21</b>	907 $\pm$ 5	3460 $\pm$ 200	18660 $\pm$ 40
<b>27</b>	860 $\pm$ 13	1104 $\pm$ 17	1408 $\pm$ 30
<b>29</b>	131 $\pm$ 1	137 $\pm$ 1	208 $\pm$ 2
<b>30</b>	1718 $\pm$ 85	1417 $\pm$ 77	1437 $\pm$ 78

<sup>a</sup>Results are the mean  $\pm$  SD of three independent experiments; nd: not determined

***In vitro* neural differentiation and maturation in the presence of various melatonin analogues.** A selection of new melatonin-based compounds covering different structural features, namely a propargyl derivative (**4**), an 1,3,4-oxadiazole (**16**), an 1,3,4-oxadiazol-2-one (**19**) and the 2-amino-1,3,4-thiadiazole (**30**), was screened at 10  $\mu$ M in primary cultures of neural stem cells. Melatonin and luzindole were also tested for comparison purposes. Neural stem cells were obtained from the SGZ of the dentate gyrus of the hippocampus of adult Wistar rats and induced to proliferate forming neurospheres (NS), as previously described.<sup>54,55</sup> The neurogenic potential of each compound was determined by direct observation of the expression of two immunostained markers, namely human  $\beta$ -tubulin III (TuJ1) and microtubule-associated protein 2 (MAP-2) and cell nuclei were identified by staining with 4',6-diamidino-2-phenylindole (DAPI). TuJ1 is expressed in neural stem cells in early stages of their differentiation, whereas the expression of MAP-2 indicates a consolidated neuronal stage.<sup>31</sup> After incubation of SGZ-NS in the presence of the compounds (10  $\mu$ M) for 7 days, they were allowed to differentiate for 48 h and finally, after immunostaining, the expression of TuJ1 and MAP-2 was visualized by fluorescence-confocal microscopy.

Figure 3 shows the neurogenic effects of new melatonin-based compounds on neural stem cell cultures. As expected, melatonin induced both early neurogenesis and cell maturation.<sup>30</sup> All melatonin analogues (**4**, **16**, **19**, and **30**) promoted the expression of TuJ1, in most cases in a larger extent than melatonin, showing also the typical neuronal morphology. Greater differences could be observed in the expression of MAP-2, 1,3,4-oxadiazole derivatives **16** and **19** being the most effective agents at stimulating cell maturation, apparently even more than melatonin itself. Surprisingly, the propargylic derivative **4**, a full agonist at both MT<sub>1</sub>R and MT<sub>2</sub>R and one of the most potent melatonergic ligands in the series, did not promote MAP-2 expression.

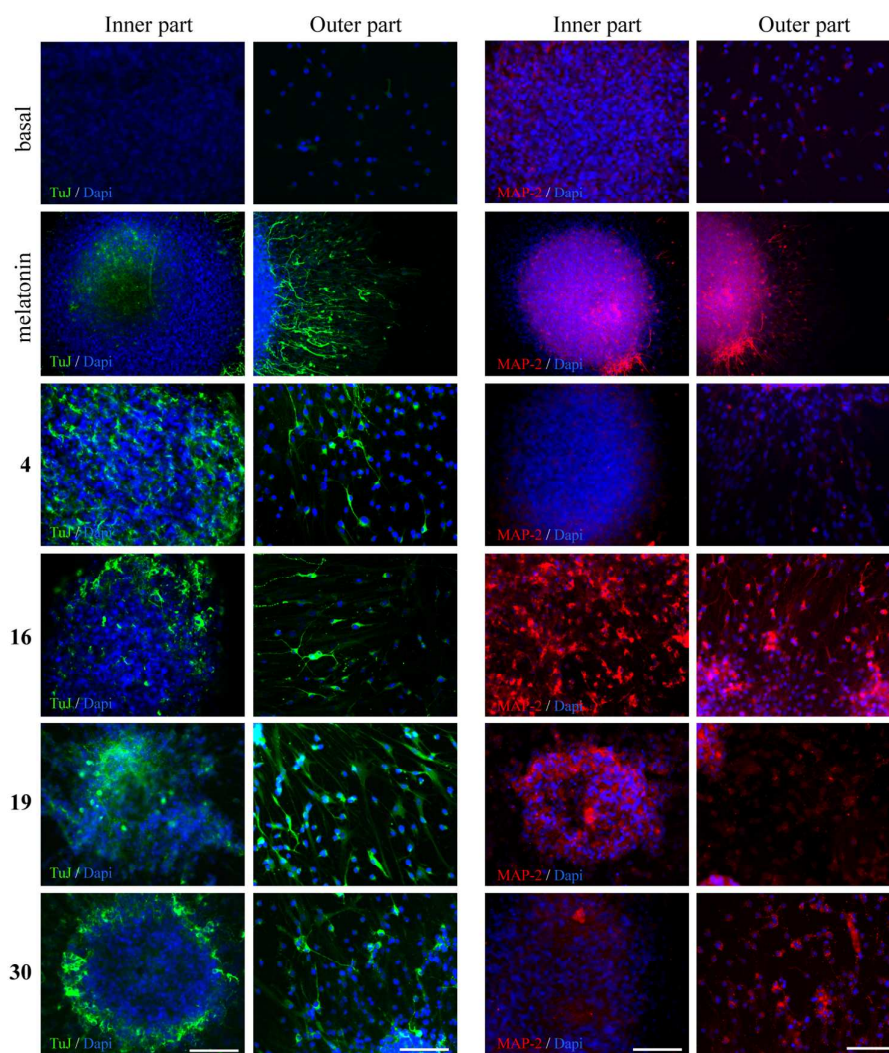


**Figure 3.** Expression of TuJ1 (green) and MAP-2 (red) in cultured SGZ-derived NS in the presence of different compounds at 10  $\mu\text{M}$ . DAPI (blue) was used as a nuclear marker. Scale bar, 200  $\mu\text{m}$ .

Melatonin, compounds **16** (the most effective at stimulating the neurogenic effect *in vitro*) and **19** (the most potent partial agonist among azoles) were further tested in the presence of the non-selective antagonist luzindole (10  $\mu$ M) to evaluate the implication of MT<sub>1</sub>R and MT<sub>2</sub>R in the expression of the neurogenic markers (Figure 4). In all three cases, preincubation with luzindole blocked the expression of both TuJ1 and MAP-2 promoted by the tested compounds, although residual expression of both TuJ1 and MAP-2 could be observed. Luzindole apparently reduced the basal expression of TuJ1 compared to the compound-free control.

According to the *in vitro* parallel artificial membrane permeability assay for the blood-brain barrier (PAMPA-BBB), the 1,3,4-oxadiazole derivative **16** showed higher passive CNS-permeability than **19** (data not shown). This non-cellular assay mimics the BBB and allows a facile high-throughput evaluation of compounds in a simplified and validated model.<sup>43,56,57</sup> Based on the results obtained in the NS studies and its positive predicted permeability in the CNS, the neurogenic profile of **16** was studied at lower concentrations (1 and 0.1  $\mu$ M). Statistical analysis showed that compound **16** stimulated the expression of TuJ1 and MAP-2 at all tested concentrations in SGZ-derived NS, in a dose-depend manner (Figure 5).

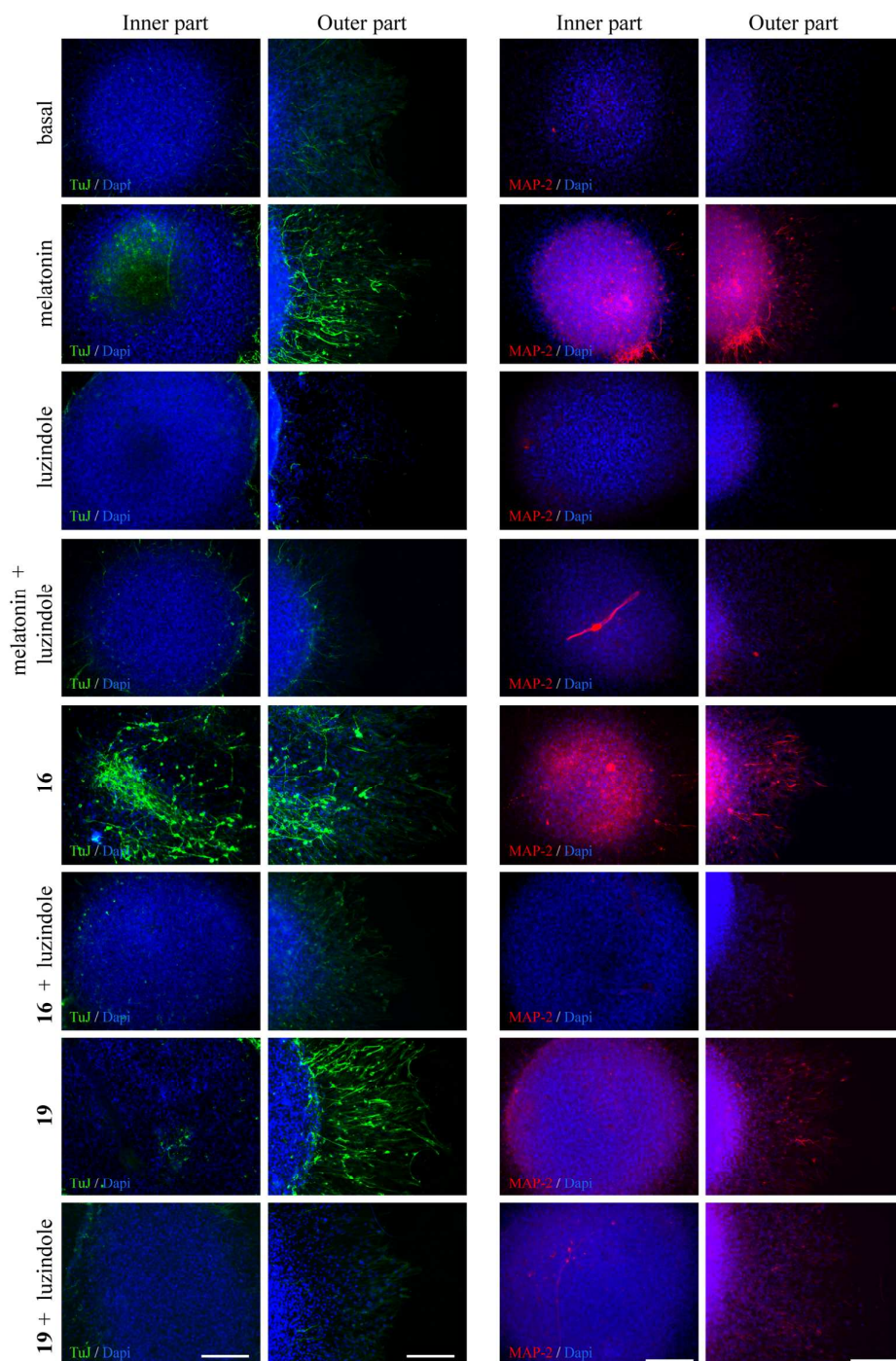


**Figure 4.** Effect of luzindole (10  $\mu$ M) on the expression of TuJ1 (green) and MAP-2 (red) promoted by melatonin, **16**, and **19** at 10  $\mu$ M in SGZ-derived NS. DAPI (blue) was used as a nuclear marker. Scale bar, 200  $\mu$ m.



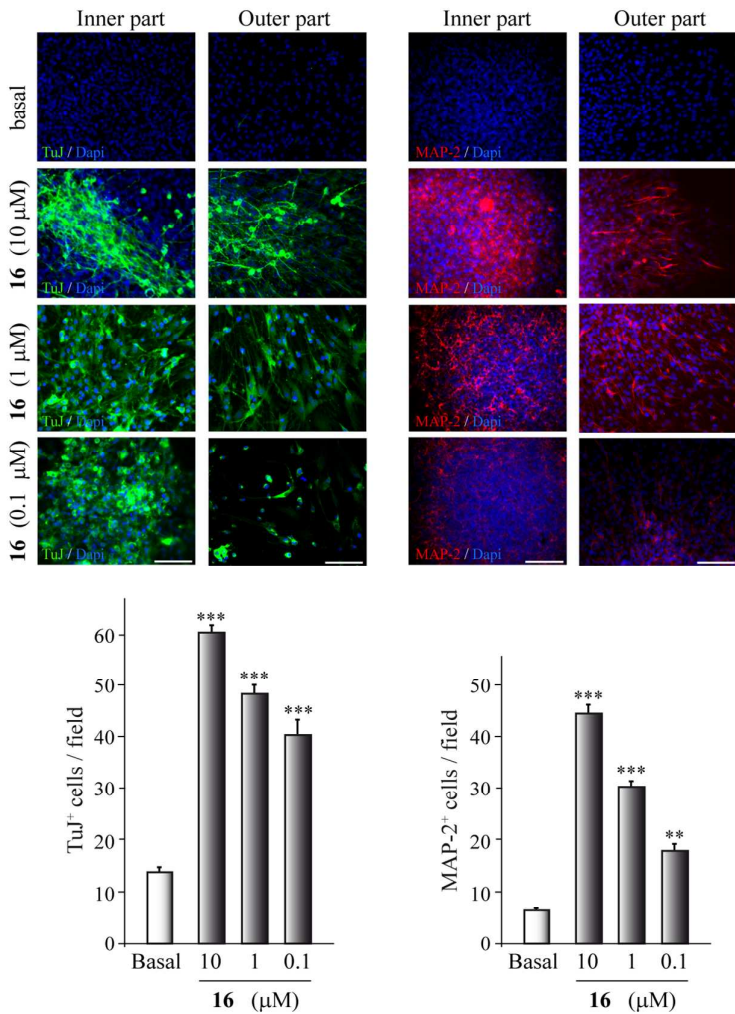


**Figure 5.** (Top) Dose-response ( $\mu$ M) effect of compound **16** on the expression of TuJ1 (green) and MAP-2 (red) in SGZ-derived NS. DAPI (blue) was used as a nuclear marker. Scale bar, 200  $\mu$ m. (Bottom) Number of TuJ1<sup>+</sup> and MAP-2<sup>+</sup> expressing cells in NS is shown and measured as the mean  $\pm$  SD. \*\*  $p \leq 0.01$ ; \*\*\*  $p \leq 0.001$ .

## DISCUSSION

Reversed amides have been already reported as a class of MTRs ligands, for instance, on the naphthalene series of agomelatine, but not yet on the classical 5-methoxyindole scaffold.<sup>19,58</sup> Binding data showing clear preference for the ethylene spacer (**4** and **6**) are consistent with literature ones. Both compounds retain good binding affinity, possibly due to the ability to arrange their pharmacophoric groups in a way resembling that of melatonin in its bioactive conformation (Figure 6).<sup>6,59</sup> This hypothesis is also supported by their full agonistic properties.

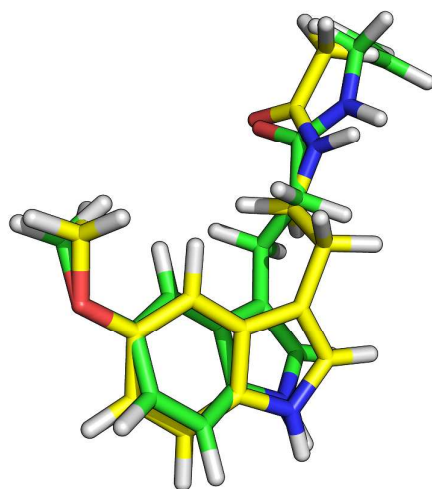


**Figure 6.** Superposition of melatonin (yellow carbons) in its putative bioactive conformation<sup>6</sup> and **6** (green carbons).

Azole derivatives binding potency was also affected by the length of the spacer; 10-fold or higher differences were found in the case of compounds bearing the same heterocycle. The preferred spacer length depends on the nature of the azole ring. In the case of the oxazoles (**7**, **8**) the spacer seems to favour the binding to a receptor subtype, but the low affinity displayed does not allow drawing any conclusions. In the case of 1,2,4- and 1,3,4-oxadiazole matching pairs, the methylene spacer is clearly favoured (**11**

/ **12**, **15** / **16**). These oxadiazole derivatives lack a hydrogen-donor centre compared to the melatonin acetamido group. Nevertheless, the hydrogen-acceptor point can be located in a nitrogen atom of the oxadiazole ring, whose relative position within the heterocycle depends on the chain length (Figure 7a).

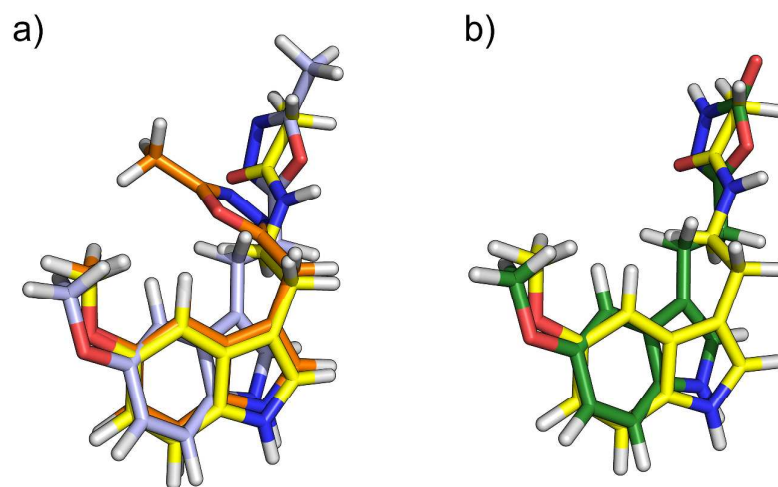


**Figure 7.** Compounds **15** (orange carbons), **16** (gray carbons) (panel a) and compound **19** (green carbons) (panel b) superposed on melatonin (yellow carbons).

Compound **17**, the nor-isomer of **16** shows the same selectivity and potency as **15**, whereas compound **16** binding is penalized in the MT<sub>2</sub>R. This penalty is probably attributable to steric clashes in the region where the amide of melatonin is accommodated, worsened by the rigid coplanar arrangement of the methyl group in the oxadiazole ring (Figure 7a).

With regard to the oxadiazole ring isomerism, the comparison between the isomer pairs **11** / **15** and **12** / **16**, assuming that each pair would bind to MTRs in a similar pose, demonstrates that the 1,3,4-oxadiazole ring is slightly preferred in terms of potency. The



isomerism of the oxadiazole does not seem to cause a change in the selectivity; the same subtle MT<sub>2</sub>R preference was observed for the azole compounds described by Rami et al.<sup>25</sup> The carbonyl group of melatonin is putatively involved in a hydrogen bond, and this moiety is necessary for binding to both receptor subtypes. On another hand, the presence of the NH from the amide group is not essential in the MT<sub>2</sub> subtype.<sup>60,61</sup> Thus, the contribution of the melatonin carbonyl group to the MT<sub>2</sub>R binding should be of greater relevance. Assuming that imine-like nitrogen within the oxadiazole ring substitutes for the carbonyl group of melatonin, the hydrogen bond acceptor properties of the heterocycle shall be crucial for MT<sub>2</sub>R recognition. Previous studies on both oxadiazole isomers revealed that calculated hydrogen bond acceptor properties of nitrogen atoms of 1,3,4-oxadiazole are greater than those of 1,2,4-oxadiazoles.<sup>26</sup> Even if the contribution of this calculated difference is limited, it could explain the preference of 1,3,4-oxadiazoles for MT<sub>2</sub>R.

In the case of acidic azoles, the affinity constants of the compounds with a methylene linker (**18**, **20**, **26**, and **28**) are all within the  $2 \cdot 10^{-7}$  -  $6 \cdot 10^{-7}$  M range for MT<sub>2</sub>R, regardless of the nature of the azole ring or the bulk of the substituents on it. Conversely, their ethylene counterparts (**19**, **21**, **27**, and **29**) showed little or no affinity for either receptor subtype, with the remarkable exception of **19** that turned out to be the most potent compound in the whole series of azoles. The 1,3,4-oxadiazolone ring of **19** can adopt two tautomeric forms, although its NMR-characterization in DMSO showed the *keto* form as the sole species. However, the acidic nature of the heterocycle, further confirmed by its differential solubility at several pHs, could also imply the existence of equilibrium with the conjugated base in aqueous media. Melatonin solubility in water is reported to be in a range between 0.4 - 0.5 mM.<sup>62,63</sup> In our experiment, the solubility of melatonin in buffer solution at pH 7.4 was found to be slightly above that range (6.64

mM, Table 3). The solubility of **19** at pH 7.4 was lower (2.10 mM), but within the same order of magnitude as melatonin. The bioisosteric replacement of the acetamido group of melatonin for 1,3,4-oxadiazolone produced a lower drop (~3-fold) in solubility than the indole-naphthalene scaffold hopping (8-fold), suggesting a comparable degree of hydrophilicity for the 1,3,4-oxadiazolone ring and the acetamide at physiological pH. It is not possible to determine the exact contribution of hydrophilicity, acidity, and plausible tautomerism to the binding affinity of compound **19** since this combination of physicochemical properties adds a great degree of complexity to the interpretation of ligand-receptor interactions within an already elusive binding pocket. Nevertheless, superimposition of **19** to the bioactive conformation of melatonin suggests that the heterocyclic nitrogen closer to the ethylene spacer can mimic the carbonyl of the amide group of melatonin (Figure 7b). Compounds **21**, **27**, and **29** could be superimposed to the structure of melatonin in a similar manner; however, none of them displayed any affinity for either MT<sub>1</sub>R or MT<sub>2</sub>R. In the case of **21**, the sulfur atom that replaces for the carbonyl-like oxygen of **19** would reasonably affect both the acidity and the probable tautomeric equilibrium in aqueous media. Moreover, this bioisosteric replacement represents an additional bulk compared to the carbonyl oxygen of **19**. All three factors could be responsible for the affinity drop of **21**. The same applies to compounds **27** and **29**, in which not only the nature of the azole is different, but also the presence of a substituent attached to it generates a greater bulk, more likely to be hindered by steric clashes within the receptor binding site.

The binding affinity constant of **30** for the MT<sub>2</sub>R is similar to those of methylene-oxadiazoles **11** and **15**, with virtually no affinity for the MT<sub>1</sub>R, showing the highest selectivity towards the MT<sub>2</sub>R of all compounds included in this work. This marked selectivity could be attributed to a differential ability of either receptor subtype to

accommodate the slightly basic ethylamino chain of **30** within their binding pockets. The selectivity profile of **30** encouraged us to increase the family of amino-thiadiazoles and amino-oxadiazoles, but unfortunately the synthetic approaches failed to provide additional analogues.

5-MeO-DMT shows a milder selectivity for the MT<sub>2</sub>R than **30**. The  $pK_a = 8.68$  of its non-methoxylated analogue, dimethyltryptamine (DMT), suggests a predominantly protonated state of 5-MeO-DMT at physiological pH.<sup>64</sup> Current knowledge of MTRs' structure is not sufficient to devise a binding mode for basic tryptamine derivatives based on experimental data. Displacement of 2-[<sup>125</sup>I]iodomelatonin by 5-MeO-DMT from hamster brain membranes was found to be 134-fold less than melatonin.<sup>28</sup> In our case, a similar decrease in affinity was found at the human MT<sub>2</sub>R subtype (100-fold). Besides its long-known agonistic properties at 5-HT receptors,<sup>65,66</sup> this methoxylated tryptamine is also able to partially activate both MTRs, being 2-fold more efficient at MT<sub>2</sub>R. This suggests an atypical case of bioisosterism in which the protonated dimethylamino group of 5-MeO-DMT can partially substitute for the uncharged amide of melatonin. Considering the hypothermic effect of melatonin,<sup>67</sup> and the similar affinities shown by 5-MeO-DMT for serotonin receptors (5-HT<sub>1A</sub>R,  $K_i = 11$  nM; 5-HT<sub>2A</sub>R,  $K_i = 92$  nM)<sup>68</sup> and human MTRs (MT<sub>1</sub>R,  $K_i = 210$  nM; MT<sub>2</sub>R,  $K_i = 16$  nM), these findings arise questions on whether the hypothermia observed in rats treated consecutively with a 5-HT<sub>2A</sub> antagonist and 5-MeO-DMT could be mediated not only via 5-HTRs, but also via MTRs.<sup>27</sup>

In contrast to the differences found in the binding affinities of all tested compounds bearing a five-membered ring, their functional profile is markedly similar and appears unaffected by the nature of the azole employed to replace the acetamido group of melatonin. While their potencies vary depending on the compound, they all retain the

mild MT<sub>2</sub>R subtype preference and are partial agonists with an  $E_{\max}$  that barely goes above the 30% of melatonin maximum response at either receptor subtype. These compounds, upon binding to MT<sub>2</sub>R, presumably fit their heterocyclic substituent in the pocket where the amide of melatonin is placed, as depicted above (exemplified for **15** and **19** in Figure 7). Nevertheless, their relatively low binding affinity suggests that either the accommodation of the azole ring in the region occupied by the acetamido group of melatonin is hampered by plausible steric clashes, or that such accommodation is secondary to some alteration in the proper arrangement of the 5-methoxyindol-3-yl-alkyl portion. Anyway, conformational changes that lead to receptor activation would be impeded, thus resulting in the observed weak partial agonism.

In the present study, we analysed the neurogenic effects of melatonin and some selected synthetic analogues *in vitro* (Figure 3), and observed that the degree of differentiation and maturation of primary neural stem cells did not correlate with their potency at MTRs (Tables 1 and 2). Compound **4** is a full agonist, weaker than melatonin at both MT<sub>1</sub>R and MT<sub>2</sub>R, yet the most potent full agonist in the series of analogues here presented. Compound **4** induces a moderate cell differentiation, but fails to stimulate neural maturation *in vitro*. In this regard, partial melatonergic agonists **16**, **19** and **30** seem to perform much better at promoting neuronal development (Figure 3). Despite its poor intrinsic activity and weak potency at MTRs, compound **16** turned out to be the most potent compound at stimulating neurogenesis *in vitro* in a dose-dependent manner (Figure 5), apparently in a greater extent than the reference compound melatonin.

In order to evaluate whether other biological pathways could be involved in the neurogenic effect of **16**, the compound was screened at 10  $\mu$ M concentration on several receptors reportedly related to neurogenesis, namely: glycogen synthase kinase 3 $\beta$  (GSK-3 $\beta$ ),<sup>69</sup> cannabinoid receptors 1 and 2 (CB<sub>1</sub>, CB<sub>2</sub>);<sup>70</sup> serotonin receptors subtype

1  
2  
3 1A, 2A, 2B, 2C (5-HT<sub>1A</sub>, 5-HT<sub>2A</sub>, 5-HT<sub>2B</sub>, 5-HT<sub>2C</sub>);<sup>71</sup> serotonin transporter (SERT);<sup>72</sup>  
4  
5 retinoic acid receptor-alpha (RAR $\alpha$ ); and peroxisome proliferator-activated receptor-  
6  
7 gamma (PPAR $\gamma$ ).<sup>73</sup> No significant interaction with the above-mentioned receptors was  
8  
9 observed.

10  
11 The fact that luzindole was unable to fully block the neural differentiation *in vitro*  
12  
13 elicited by melatonin has already been observed by Ramírez-Rodríguez et al.<sup>30</sup> The  
14  
15 residual expression of TuJ1 stimulated by melatonin, **16**, and **19** in the presence of  
16  
17 luzindole (Figure 4) could be related to the interaction of these compounds with other  
18  
19 systems. Indeed, melatonin has also been reported to interact with nuclear receptors  
20  
21 from the retinoic acid superfamily, not related to MT<sub>1</sub>R and MT<sub>2</sub>R signalling  
22  
23 pathways.<sup>74</sup>  
24  
25  
26

27 Although luzindole is unable to counteract totally the effects of melatonin, **16**, or  
28  
29 **19**, interestingly it blocks the basal neural differentiation below its constitutive levels as  
30  
31 observed in the TuJ1 expression *in vitro* (Figure 4). This effect has already been  
32  
33 described and could be related to the nature of luzindole, a pure antagonist at MT<sub>2</sub>R and  
34  
35 an inverse agonist at MT<sub>1</sub>R.<sup>30,75</sup> Both receptor subtypes can be found in the dentate  
36  
37 gyrus of rat hippocampus.<sup>76</sup> Luzindole ability to decrease melatonergic intrinsic activity  
38  
39 below its constitutive level could block, or partially block, other intracellular pathways  
40  
41 via signalling cross-talk, reducing basal neural differentiation. The magnitude of this  
42  
43 observed effect is rather low at basal levels, although it could be of relevance in the case  
44  
45 of neural differentiation elicited by compound **16**. Taking into account the low potency  
46  
47 of **16** at MTRs, a hypothetical neurogenic contribution beyond MT<sub>1</sub>R and/or MT<sub>2</sub>R  
48  
49 could be partially masked by a negative cross-talk.  
50  
51  
52  
53

54 The blockade exerted by luzindole on the neurogenic actions of melatonin, **16**, and  
55  
56 **19** *in vitro* suggests the involvement of MT<sub>1</sub>R and/or MT<sub>2</sub>R. It is surprising how weak  
57  
58  
59  
60

partial agonists like **16** and **19**, barely able to stimulate the MTRs activation ( $\leq 30\%$  relative intrinsic activity in the [ $^{35}\text{S}$ ]GTP $\gamma$ S assay, see Table 2), are potent neurogenic agents *in vitro*. To gain insights at this point, additional functional assays were carried out with **16** and **19**; their intrinsic activities at MTRs were measured as impedance in the case of MT<sub>1</sub>R and as decrease of cAMP levels in the case of MT<sub>2</sub>R.<sup>77,78</sup> Summarizing the results, **16** was too weak to elicit any measurable stimulation of the MT<sub>1</sub>R, whereas it reached a full agonist response at the MT<sub>2</sub>R ( $EC_{50} = 1.6 \mu\text{M}$ ;  $E_{\text{max}} = 92\%$ ). Compound **19** behaved as a full agonist at both MT<sub>1</sub>R ( $EC_{50} = 48 \text{ nM}$ ;  $E_{\text{max}} = 100\%$ ) and MT<sub>2</sub>R ( $EC_{50} = 5.5 \text{ nM}$ ;  $E_{\text{max}} = 97\%$ ). A plausible hypothesis to explain these observed amplification effects is functional selectivity.<sup>79</sup> This phenomenon is quite ubiquitous in GPCRs, and MTRs are known to couple to several G-proteins, with special preference for G<sub>i</sub> proteins, that upon dissociation could differentially activate parallel pathways.<sup>74</sup> The [ $^{35}\text{S}$ ]GTP $\gamma$ S assay is unable to discriminate between different G-proteins but the preferential activation of certain MT<sub>n</sub>R-G-protein populations would provoke the activation of their coupled signalling pathways, and thus only their mediated effects would be observed (Figure 8). These findings are insufficient to establish a plausible hypothesis for the observed neurogenic effect; however, they appear to suggest a distinctive activation mechanism of MTRs by azole derivatives.

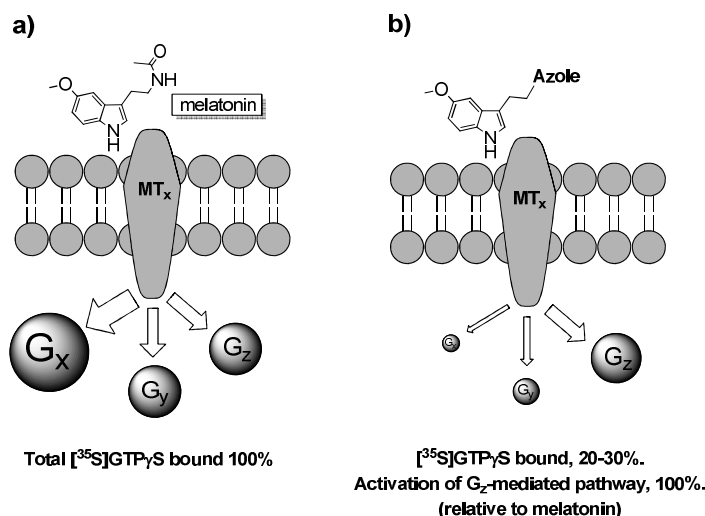


**Figure 8.** Schematic representation of the functional selectivity hypothesis of melatonin-azole derivatives at MTRs. (Panel a) Melatonin, the reference and native ligand, binds to MTRs coupled to G-proteins, that upon activation bind [<sup>35</sup>S]GTPγS. The amount of G-protein activated is taken arbitrarily as 100%. The size and names of the G-proteins are fictional and represent the relative population of certain activated G-protein isoforms. (Panel b) The low binding of [<sup>35</sup>S]GTPγS upon binding of melatonin-azole derivatives to MTRs could indicate the preferential activation of certain populations of MT<sub>n</sub>-G<sub>n</sub>, and subsequently, of their corresponding signalling pathways.

## Conclusions

A new family of neurogenic melatonin-based drugs, covered by a PCT patent,<sup>80</sup> has been obtained. Maintaining the 5-methoxyindole nucleus intact we have bioisosterically replaced the acetamido group of melatonin by different reversed amides and azoles and characterized their binding affinity and functional behaviour at MT<sub>1</sub>R and MT<sub>2</sub>R. The retroamide replacement proved to be the best approach, yielding potent agonists at both MTR subtypes. In the case of oxadiazoles, both 1,3,4- and 1,2,4-isomers could substitute for the acetamido moiety, retaining the ability to bind to MTRs. Pharmacological and physicochemical properties of compound **19** allowed to identify the 1,3,4-oxadiazol-2-one ring as a promising starting point for further structure-activity relationship studies that could help to the understanding of the molecular recognition events occurring between MT<sub>1</sub>R and MT<sub>2</sub>R and the acetamido group of melatonin.

Furthermore, we have investigated the neurogenic properties of several of the abovementioned melatonin analogues *in vitro*. Even if MTRs seemingly appear implicated in mediating this effect --effectively blocked by luzindole in the case of melatonin, **16**, and **19**-- its magnitude does not correlate with compounds' potency at MT<sub>1</sub>R and MT<sub>2</sub>R. Such discrepancy could be possibly related to a functional selectivity phenomenon, or to interactions with additional pathways not directly related to the MT<sub>1</sub>R or MT<sub>2</sub>R activation, but affected by their blockade. Taking into account these observations, melatonin-azole derivatives behave as full melatonin bioisosteres in the phenotypical promotion of neurogenesis *in vitro*, well beyond their reduced ability to substitute for melatonin at MTRs. Considering its neurogenic profile, solubility and predicted CNS-permeability, we propose 2-(2-(5-methoxy-1*H*-indol-3-yl)ethyl)-5-methyl-1,3,4-oxadiazole (**16**) as a useful candidate for further development in the search for reparative agents for CNS-diseases.



## EXPERIMENTAL SECTION

**Chemistry. General Methods.** Reagents and solvents were purchased from common commercial suppliers, mostly Sigma-Aldrich, and were used without further purification. 5-MeO-DMT was synthesized according to literature procedure.<sup>81</sup> Analytical thin-layer chromatography (TLC) was carried out using Merck silica gel 60 F254 plates, and the compounds were visualized under UV-light ( $\lambda = 254$  or  $365$  nm) and/or stained with phosphomolybdic acid 10% wt. in ethanol. Automatized chromatographic separation was carried out in an IsoleraOne (Biotage) equipment, using different silica Si<sub>50</sub> cartridges from Agilent Technologies. High-performance liquid chromatography was performed on a Waters analytical HPLC-MS (Alliance Waters 2690) equipped with a SunFire C<sub>18</sub> 4.6 x 50 mm column, a UV photodiode array detector ( $\lambda = 214$ – $274$  nm) and quadrupole mass spectrometer (Micromass ZQ). HPLC analyses were used to confirm the purity of all compounds ( $\geq 95\%$ ) and were performed on Waters 6000 equipment, at a flow rate of 1.0 mL/min, with a UV photodiode array detector ( $\lambda = 214$ – $274$  nm), and using a Delta Pak C<sub>18</sub> 5  $\mu$ m, 300 Å column. The elution was performed in a gradient mixture of MeCN/water.

Melting points (uncorrected) were determined in a MP70 apparatus (Mettler Toledo). <sup>1</sup>H NMR and <sup>13</sup>C NMR spectra were recorded in CDCl<sub>3</sub>, DMSO-*d*<sub>6</sub>, or acetone-*d*<sub>6</sub> solutions using the following NMR spectrometers: Varian INOVA-300, Varian INOVA-400, Varian Mercury-400 or Varian Unity-500. Chemical shifts are reported in  $\delta$  scale (ppm) relative to internal Me<sub>4</sub>Si. *J* values are given in hertz, and spin multiplicities are expressed as s (singlet), d (doublet), t (triplet), q (quartet), or m (multiplet). High Resolution Mass Spectra (HRMS) were obtained by electron spray ionization in positive mode (ESI<sup>+</sup>) using a Hewlett-Packard MSD 1100 spectrometer.

**General Procedure for the Synthesis of Propargyl- or Allyl- Amides (3-6).** The corresponding acid (1 mmol) was dissolved in dry acetonitrile (MeCN, 20 mL) and then CDI, (1.2 mmol) and a catalytic amount of dimethylaminopyridine (DMAP, 0.01 mmol) were added. After stirring for 2 h at 50 °C, the corresponding unsaturated amine (1 mmol) was added to the solution and the mixture was stirred for an additional 2 h period at room temperature (rt). Then, solvent was evaporated to dryness and crude was treated with HCl 1M (20 mL), and the resulting suspension was extracted with ethyl acetate (EtOAc, 3 x 20 mL). The combined organic layers were washed with NaOH 2M (3 x 20 mL), dried over anhydrous MgSO<sub>4</sub>, and evaporated to dryness in vacuo to yield the corresponding propargyl- or allyl- amide.

***N*-Propargyl-2-(5-methoxy-1*H*-indol-3-yl)-acetamide (3).** According to the general procedure, from 2-(5-methoxy-1*H*-indol-3-yl)acetic acid (200 mg, 1.0 mmol) and propargylamine (0.64 mL, 1.0 mmol), **3** (146 mg, 61%) was obtained as a white solid of mp: 117 – 118 °C. <sup>1</sup>H NMR (500 MHz, DMSO) δ 10.70 (s, 1H), 8.33 (t, *J* = 5.5 Hz, 1H), 7.22 (d, *J* = 8.7 Hz, 1H), 7.13 (d, *J* = 2.4 Hz, 1H), 7.04 (d, *J* = 2.4 Hz, 1H), 6.71 (dd, *J* = 8.7, 2.5 Hz, 1H), 3.85 (dd, *J* = 5.5, 2.5 Hz, 2H), 3.75 (s, 3H), 3.47 (s, 2H), 3.08 (t, *J* = 2.5 Hz, 1H). <sup>13</sup>C NMR (126 MHz, DMSO-*d*<sub>6</sub>) δ 170.91, 153.45, 131.65, 127.93, 124.87, 112.36, 111.53, 108.73, 100.99, 81.81, 73.26, 55.79, 32.93, 28.39. HRMS (ESI<sup>+</sup>): *m/z* calcd for C<sub>14</sub>H<sub>14</sub>N<sub>2</sub>O<sub>2</sub> (M)<sup>+</sup> 242.1055, found 242.1063. HPLC purity 100% (230 to 400 nm).

***N*-Propargyl-3-(5-methoxy-1*H*-indol-3-yl)-propanamide (4).** Following the general procedure, from 3-(5-methoxy-1*H*-indol-3-yl)propanoic acid (219 mg, 1.0 mmol) and propargylamine (0.71 mL, 1.1 mmol), **4** (167 mg, 65%) was obtained as a white solid of mp: 118 – 119 °C. <sup>1</sup>H NMR (300 MHz, acetone-*d*<sub>6</sub>) δ 7.25 (d, *J* = 8.8 Hz, 1H), 7.12 –

7.04 (m, 2H), 6.74 (dd,  $J = 8.8, 2.5$  Hz, 1H), 3.98 (d,  $J = 2.6$  Hz, 2H), 3.80 (s, 3H), 3.02 (t,  $J = 7.7$  Hz, 2H), 2.61 (t,  $J = 2.6$  Hz, 1H), 2.56 (m, 2H).  $^{13}\text{C}$  NMR (75 MHz, acetone)  $\delta$  173.16, 155.26, 133.31, 129.32, 124.06, 115.76, 113.29, 112.93, 101.79, 82.19, 72.44, 56.54, 37.93, 29.38, 22.54. HRMS (ESI<sup>+</sup>):  $m/z$  calcd for  $\text{C}_{15}\text{H}_{16}\text{N}_2\text{O}_2$  (M)<sup>+</sup> 256.1212, found 256.1202. HPLC purity 97% (230 to 400 nm).

***N*-Allyl-2-(5-methoxy-1*H*-indol-3-yl)acetamide (5).** According to the general procedure, from 2-(5-methoxy-1*H*-indol-3-yl)acetic acid (168 mg, 0.84 mmol) and allylamine (92  $\mu\text{L}$ , 1.26 mmol), **5** (178 mg, 86%) was obtained as a yellow oil that crystallised upon standing. Mp: 92 – 93 °C.  $^1\text{H}$  NMR (300 MHz, DMSO)  $\delta$  10.69 (s, 1H), 8.05 – 7.97 (m, 1H), 7.21 (d,  $J = 8.7$  Hz, 1H), 7.13 (d,  $J = 2.2$  Hz, 1H), 7.06 (d,  $J = 2.4$  Hz, 1H), 6.70 (dd,  $J = 8.7, 2.4$  Hz, 1H), 5.77 (ddt,  $J = 17.1, 10.3, 5.2$  Hz, 1H), 5.08 (dd,  $J = 17.1, 1.8$  Hz, 1H), 5.00 (dd,  $J = 10.3, 1.8$  Hz, 1H), 3.73 (s, 3H), 3.68 (m, 2H), 3.48 (s, 2H).  $^{13}\text{C}$  NMR (75 MHz, DMSO)  $\delta$  170.51, 152.96, 135.49, 131.21, 127.49, 124.42, 114.85, 111.90, 111.04, 108.61, 100.53, 55.30, 40.90, 32.70. HRMS (ESI<sup>+</sup>):  $m/z$  calcd for  $\text{C}_{14}\text{H}_{16}\text{N}_2\text{O}_2$  (M)<sup>+</sup> 244.1212, found 244.1202. HPLC purity 100% (230 to 400 nm).

***N*-Allyl-3-(5-methoxy-1*H*-indol-3-yl)propanamide (6).** Following the general procedure, from 3-(5-methoxy-1*H*-indol-3-yl)propanoic acid (80 mg, 0.36 mmol) and allylamine (40  $\mu\text{L}$ , 0.54 mmol), **6** (81 mg, 87%) was obtained as a brownish solid of mp: 173 – 174 °C.  $^1\text{H}$  NMR (300 MHz, DMSO)  $\delta$  10.58 (s, 1H), 7.99 (t,  $J = 5.1$  Hz, 1H), 7.21 (d,  $J = 8.7$  Hz, 1H), 7.05 (d,  $J = 2.1$  Hz, 1H), 7.00 (d,  $J = 2.4$  Hz, 1H), 6.71 (dd,  $J = 8.7, 2.4$  Hz, 1H), 5.77 (ddt,  $J = 17.2, 10.4, 5.2$  Hz, 1H), 5.08 (dd,  $J = 17.3, 1.8$  Hz, 1H), 5.02 (dd,  $J = 10.3, 1.7$  Hz, 1H), 3.76 (s, 3H), 3.70 (t,  $J = 5.5$  Hz, 2H), 2.89 (t,  $J = 7.5$  Hz, 2H), 2.45 (t,  $J = 7.5$  Hz, 2H).  $^{13}\text{C}$  NMR (75 MHz, DMSO)  $\delta$  172.08, 153.25, 135.88, 131.73, 127.67, 123.14, 115.31, 113.98, 112.25, 111.34, 100.62, 55.72, 41.18,

36.48, 21.44. HRMS (ESI<sup>+</sup>): *m/z* calcd for C<sub>15</sub>H<sub>18</sub>N<sub>2</sub>O<sub>2</sub> (M)<sup>+</sup> 258.1368, found 258.1370. HPLC purity 100% (230 to 400 nm).

**Synthesis of Oxazoles. 2-((5-Methoxy-1*H*-indol-3-yl)methyl)-5-methyloxazole (7).**

To a solution of **3** (100 mg, 0.41 mmol) in 10 mL of dry dichloromethane, gold(III) chloride (12 mg, 0.041 mmol) was added and the resulting mixture was stirred at rt for 18 h under inert atmosphere. After this time, TEA (0.5 mL) was added and the reaction mixture was filtered over a short plug of silica gel eluting with EtOAc. Solvent was evaporated to dryness and the resulting oil was chromatographed on silica gel (gradient hexane: EtOAc) to afford **7** (18 mg, 18%) as a coloured solid of mp: 106 – 108 °C. <sup>1</sup>H NMR (300 MHz, CDCl<sub>3</sub>) δ 8.35 (s, 1H), 7.25 (d, *J* = 8.8 Hz, 1H), 7.17 – 7.05 (m, 2H), 6.85 (dd, *J* = 8.8, 2.5 Hz, 1H), 6.66 (s, 1H), 4.21 (s, 2H), 3.85 (s, 3H), 2.26 (s, 3H). <sup>13</sup>C NMR (101 MHz, CDCl<sub>3</sub>) δ 161.52, 154.30, 144.90, 131.45, 127.62, 123.57, 122.55, 112.74, 112.03, 110.12, 100.77, 56.02, 25.07, 11.08. HRMS (ESI<sup>+</sup>): *m/z* calcd for C<sub>14</sub>H<sub>14</sub>N<sub>2</sub>O<sub>2</sub> (M)<sup>+</sup> 242.1055, found 242.1055. HPLC purity 100% (230 to 400 nm).

**2-(2-(5-Methoxy-1*H*-indol-3-yl)ethyl)-5-methyloxazole (8).** Starting from **4** (30 mg, 0.11 mmol), this derivative was synthesized according to the procedure described for **7**, obtaining **8** (11 mg, 38%) as a light brown solid of mp: 100 – 105 °C. <sup>1</sup>H NMR (300 MHz, CDCl<sub>3</sub>) δ 7.94 (s, 1H), 7.25 (d, *J* = 8.8 Hz, 1H), 7.03 (d, *J* = 2.3 Hz, 1H), 7.00 (s, 1H), 6.86 (dd, *J* = 8.8, 2.3 Hz, 1H), 6.64 (s, 1H), 3.87 (s, 3H), 3.23-3.18 (m, 1H), 3.13-3.08 (m, 1H), 2.28 (s, 3H). <sup>13</sup>C NMR (101 MHz, CDCl<sub>3</sub>) δ 163.51, 154.08, 148.39, 131.48, 127.72, 122.53, 122.31, 114.90, 112.45, 111.98, 100.54, 56.06, 29.03, 22.97, 11.01. HRMS (ESI<sup>+</sup>): *m/z* calcd for C<sub>15</sub>H<sub>16</sub>N<sub>2</sub>O<sub>2</sub> (M)<sup>+</sup> 256.1212, found 256.1209. HPLC purity 95% (230 to 400 nm).

**Synthesis of Esters. Ethyl 2-(5-methoxy-1*H*-indol-3-yl)acetate (9).**<sup>82</sup> To a solution of 2-(5-methoxy-1*H*-indol-3-yl)acetic acid (3.5 g, 17.07 mmol) in 50 mL of EtOH 25

drops of concentrated sulfuric acid were added. The mixture was heated under reflux for 2 h, cooled to rt, neutralized with a solution of NaOH 2M, and evaporated to dryness in vacuo. The residue was treated with water (40 mL) and extracted with EtOAc (3 x 40 mL). Removal of the organic solvent under reduced pressure gave **9** (3.42 mg, 86%) as a light yellow solid. <sup>1</sup>H NMR (300 MHz, DMSO) δ 10.77 (s, 1H), 7.23 (d, *J* = 8.7 Hz, 1H), 7.19 (d, *J* = 2.3 Hz, 1H), 6.98 (d, *J* = 2.4 Hz, 1H), 6.72 (dd, *J* = 8.7, 2.4 Hz, 1H), 4.07 (q, *J* = 7.1 Hz, 2H), 3.74 (s, 3H), 3.68 (s, 2H), 1.18 (t, *J* = 7.1 Hz, 3H). <sup>13</sup>C NMR (75 MHz, DMSO) δ 171.52, 153.06, 131.19, 127.38, 124.61, 112.04, 111.19, 106.75, 100.27, 59.98, 55.26, 30.89, 14.14. HPLC-MS (230 to 400 nm) 100% (*m/z*) [*MH*<sup>+</sup>] 234.44.

**Ethyl 3-(5-methoxy-1*H*-indol-3-yl)propanoate (10).**<sup>83</sup> To a solution of 5-methoxy-1*H*-indole (5.0 g, 34 mmol) and ethyl acrylate (21.7 mL, 0.2 mol) in DCM (40 mL), anhydrous ZrCl<sub>4</sub> (1.0 g, 4.29 mmol) was added and the mixture was kept stirring at rt for 18 h. Then, the catalyst was filtered off and the solvent and excess of ethyl acrylate were removed under vacuum and collected in a cold trap. The resulting crude was chromatographed on silica gel (gradient DCM: MeOH) to afford **10** (6.1 g, 71%) as a white pearly solid. <sup>1</sup>H NMR (300 MHz, CDCl<sub>3</sub>) δ 7.88 (s, 1H), 7.24 (d, *J* = 8.8 Hz, 1H), 7.04 (d, *J* = 2.3 Hz, 1H), 6.99 (s, 1H), 6.86 (dd, *J* = 8.8, 2.3 Hz, 1H), 4.15 (q, *J* = 7.1 Hz, 2H), 3.87 (s, 3H), 3.07 (t, *J* = 7.6 Hz, 2H), 2.71 (t, *J* = 7.6 Hz, 2H), 1.25 (t, *J* = 7.1 Hz, 3H). <sup>13</sup>C NMR (75 MHz, CDCl<sub>3</sub>) δ 173.40, 153.93, 131.38, 127.55, 122.12, 114.77, 112.22, 111.77, 100.56, 60.32, 55.92, 34.81, 20.60, 14.19. HPLC-MS (230 to 400 nm) 100% (*m/z*) [*MH*<sup>+</sup>] 248.06.

**Synthesis of 1,2,4-Oxadiazoles. 5-((5-Methoxy-1*H*-indol-3-yl)methyl)-3-methyl-1,2,4-oxadiazole (11).** Acetamidoxime (95 mg, 1.3 mmol), 1.5 g of molecular sieves (3Å), and sodium hydride (61 mg, 2.5 mmol) were suspended in anhydrous THF (4 mL)

and stirred at 50 °C. After stirring for 2 h, **9** (150 mg, 0.64 mmol) dissolved in THF (2 mL) was slowly added to the mixture that was kept with gentle stirring for additional 18 h. Then, the mixture was filtered and the solids washed with EtOAc (10 mL). The filtrate was evaporated under vacuum and the crude was chromatographed on silica gel (gradient DCM: MeOH) to afford **11** (87 mg, 56%) as a brownish solid of mp: 100 – 102 °C. <sup>1</sup>H NMR (300 MHz, CDCl<sub>3</sub>) δ 8.07 (s, 1H), 7.28-7.25 (m, 1H), 7.21 (s, 1H), 7.05 (d, *J* = 2.4 Hz, 1H), 6.88 (dd, *J* = 8.8, 2.4 Hz, 1H), 4.32 (s, 2H), 3.87 (s, 3H), 2.38 (s, 3H). <sup>13</sup>C NMR (75 MHz, CDCl<sub>3</sub>) δ 178.54, 167.55, 154.68, 131.54, 127.45, 124.04, 113.20, 112.36, 108.07, 100.63, 56.19, 23.56, 11.91. HRMS (ESI<sup>+</sup>): *m/z* calcd for C<sub>13</sub>H<sub>13</sub>N<sub>3</sub>O<sub>2</sub> (M)<sup>+</sup> 243.1017, found 243.1008. HPLC purity 100% (230 to 400 nm).

**5-(2-(5-Methoxy-1*H*-indol-3-yl)ethyl)-3-methyl-1,2,4-oxadiazole (12).** Starting from **10** (173 mg, 0.7 mmol), the compound was synthesized according to the procedure described for **11**, obtaining **12** (80 mg, 45%) as an off-white solid of mp: 75 – 76 °C. <sup>1</sup>H NMR (400 MHz, DMSO) δ 10.66 (s, 1H), 7.21 (d, *J* = 8.7 Hz, 1H), 7.09 (d, *J* = 2.4 Hz, 1H), 6.99 (d, *J* = 2.4 Hz, 1H), 6.71 (dd, *J* = 8.7, 2.4 Hz, 1H), 3.76 (s, 3H), 3.23 (t, *J* = 7.3 Hz, 2H), 3.12 (t, *J* = 7.3 Hz, 2H), 2.30 (s, 3H). <sup>13</sup>C NMR (100 MHz, DMSO) δ 180.04, 167.35, 153.71, 131.95, 127.73, 123.90, 112.82, 112.73, 111.95, 100.54, 55.99, 27.40, 22.58, 11.80. HRMS (ESI<sup>+</sup>): *m/z* calcd for C<sub>14</sub>H<sub>15</sub>N<sub>3</sub>O<sub>2</sub> (M)<sup>+</sup> 257.1164, found 257.1172. HPLC purity 100% (230 to 400 nm).

**Synthesis of hydrazides. 2-(5-Methoxy-1*H*-indol-3-yl)acetohydrazide (13).**<sup>84</sup> A mixture of **9** (1.53 g, 6.5 mmol) and excess of hydrazine hydrate (5 mL) in EtOH (6 mL) was heated to 155 °C for 45 min under microwave irradiation. After removing the solvent, the milky crude was resuspended in water (70 mL) and extracted with EtOAc (6 x 50 mL). The organic extracts were dried over anhydrous magnesium sulfate and solvent removed to give **13** (1.40 g, 98%) as a white solid. <sup>1</sup>H NMR (300 MHz, DMSO)

$\delta$  10.76 (s, 1H), 9.09 (s, 1H), 7.20 (d,  $J$  = 8.7 Hz, 1H), 7.12 (d,  $J$  = 2.3 Hz, 1H), 7.06 (d,  $J$  = 2.4 Hz, 1H), 6.69 (dd,  $J$  = 8.7, 2.4 Hz, 1H), 4.17 (s, 2H), 3.74 (s, 3H), 3.39 (s, 2H).  $^{13}\text{C}$  NMR (75 MHz, DMSO)  $\delta$  170.13, 152.94, 131.16, 127.48, 124.31, 111.83, 110.92, 108.41, 100.71, 55.35, 30.74. HPLC-MS (230 to 400 nm) 100% ( $m/z$ ) [ $\text{MH}^+$ ] 220.11.

**3-(5-Methoxy-1*H*-indol-3-yl)propanehydrazide (14).** Starting from **10** (3.0 g, 12.1 mmol), this compound was synthesized according to the procedure described for **13**, obtaining **14** (2.8 g, 100%) as an off-white solid.  $^1\text{H}$  NMR (300 MHz, DMSO)  $\delta$  10.59 (s, 1H), 9.00 (s, 1H), 7.20 (d,  $J$  = 8.7 Hz, 1H), 7.04 (d,  $J$  = 2.2 Hz, 1H), 6.98 (d,  $J$  = 2.4 Hz, 1H), 6.70 (dd,  $J$  = 8.7, 2.4 Hz, 1H), 4.18 (s, 2H), 3.76 (s, 3H), 2.87 (t,  $J$  = 8.0 Hz, 2H), 2.37 (t,  $J$  = 8.0 Hz, 2H). HPLC-MS (230 to 400 nm) 96% ( $m/z$ ) [ $\text{MH}^+$ ] 234.08.

**General procedure for the Synthesis of 1,3,4-Oxadiazoles.** The corresponding hydrazide (0.5 mmol) was suspended in an excess of an orthoester (1 mL) and a catalytic amount of acetic acid (1 drop) was added. The mixture was heated in a microwave system for 1 h at 125 °C. Then, the excess of the orthoester was evaporated to dryness and the crude chromatographed on silica gel (gradient DCM:MeOH), obtaining the corresponding 1,3,4-oxadiazole.

**2-((5-Methoxy-1*H*-indol-3-yl)methyl)-5-methyl-1,3,4-oxadiazole (15).** According to the above general procedure, from **13** (100 mg, 0.45 mmol), triethyl orthoacetate (1 mL) and a catalytic amount of acetic acid, **15** (71 mg, 64%) was obtained as a brownish solid of mp: 139 – 140 °C.  $^1\text{H}$  NMR (300 MHz,  $\text{CDCl}_3$ )  $\delta$  8.33 (s, 1H), 7.25 (d,  $J$  = 8.8 Hz, 1H), 7.14 (s, 1H), 7.06 (d,  $J$  = 2.3 Hz, 1H), 6.86 (dd,  $J$  = 8.8, 2.3 Hz, 1H), 4.27 (s, 2H), 3.84 (s, 3H), 2.44 (s, 3H).  $^{13}\text{C}$  NMR (75 MHz,  $\text{CDCl}_3$ )  $\delta$  165.95, 163.93, 154.25, 131.26, 127.15, 123.78, 112.75, 112.09, 107.86, 100.24, 55.85, 22.09, 10.94. HRMS ( $\text{ESI}^+$ ):  $m/z$  calcd for  $\text{C}_{13}\text{H}_{13}\text{N}_3\text{O}_2$  ( $\text{M}$ ) $^+$  243.1008, found 243.1017. HPLC purity 100% (230 to 400 nm).

**2-(2-(5-Methoxy-1*H*-indol-3-yl)ethyl)-5-methyl-1,3,4-oxadiazole (16).** Following the general procedure, from **14** (405 mg, 1.74 mmol), triethyl orthoacetate (3.5 mL) and a catalytic amount of acetic acid, derivative **16** (257 mg, 57%) was obtained as a brownish solid of mp: 156 – 157 °C. <sup>1</sup>H NMR (300 MHz, CDCl<sub>3</sub>) δ 8.03 (s, 1H), 7.91 (s, 1H), 7.25 (d, *J* = 8.8 Hz, 1H), 7.01 (s, 1H), 6.99 (d, *J* = 2.4 Hz, 1H), 6.87 (dd, *J* = 8.8, 2.4 Hz, 1H), 3.87 (s, 3H), 3.24 – 3.20 (m, 4H), 2.47 (s, 3H). <sup>13</sup>C NMR (75 MHz, CDCl<sub>3</sub>) δ 166.79, 163.64, 154.05, 131.37, 127.39, 122.40, 113.78, 112.34, 111.95, 100.28, 55.93, 26.17, 22.34, 10.90. HRMS (ESI<sup>+</sup>): *m/z* calcd for C<sub>14</sub>H<sub>15</sub>N<sub>3</sub>O<sub>2</sub> (M)<sup>+</sup> 257.1164, found 257.1158. HPLC purity 100% (230 to 400 nm).

**2-(2-(5-Methoxy-1*H*-indol-3-yl)ethyl)-1,3,4-oxadiazole (17).** According to the above general procedure, from **14** (120 mg, 0.5 mmol), trimethyl orthoformate (1 mL) and a catalytic amount of acetic acid, compound **17** (41 mg, 34%) was obtained as an off-white solid of mp: 148 – 149 °C. <sup>1</sup>H NMR (300 MHz, DMSO) δ 9.73 (s, 1H), 8.40 (s, 1H), 7.18 (d, *J* = 8.8 Hz, 1H), 6.92 (d, *J* = 2.5 Hz, 1H), 6.87 (d, *J* = 2.5 Hz, 1H), 6.71 (dd, *J* = 8.7, 2.5 Hz, 1H), 3.76 (s, 3H), 3.23 – 3.14 (m, 4H). <sup>13</sup>C NMR (75 MHz, DMSO) δ 165.54, 152.51, 152.08, 130.55, 126.06, 121.78, 111.40, 111.15, 110.63, 98.79, 54.71, 24.99, 21.28. HRMS (ESI<sup>+</sup>): *m/z* calcd for C<sub>13</sub>H<sub>13</sub>N<sub>3</sub>O<sub>2</sub> (M)<sup>+</sup> 243.1008, found 243.1014. HPLC purity 98% (230 to 400 nm).

**Synthesis of 1,3,4-oxadiazol-2-(thio)ones. 5-((5-Methoxy-1*H*-indol-3-yl)methyl)-1,3,4-oxadiazol-2(3*H*)-one (18).** A mixture of **13** (86 mg, 0.4 mmol), CDI (76 mg, 0.47 mmol), TEA (0.11 mL, 0.8 mmol) dissolved in THF was heated to 100 °C for 15 min. Solvent was evaporated and the residue was treated with a small amount of water (2 mL), basified to pH 12-13 with NaOH (conc.) and filtered. The filtrate was collected and acidified with HCl (conc.) and thus, the compound precipitated. The precipitate was filtered off to afford **18** (72 mg, 73%) as a pearly white solid of mp 140 – 141 °C. <sup>1</sup>H



NMR (300 MHz, DMSO)  $\delta$  12.08 (s, 1H), 10.89 (s, 1H), 7.26 (d,  $J$  = 8.8 Hz, 1H), 7.24 (s, 1H), 7.00 (d,  $J$  = 2.4 Hz, 1H), 6.74 (dd,  $J$  = 8.8, 2.4 Hz, 1H), 3.97 (s, 2H), 3.73 (s, 3H).  $^{13}\text{C}$  NMR (75 MHz, DMSO)  $\delta$  156.46, 155.07, 153.18, 131.24, 127.03, 124.78, 112.22, 111.27, 105.87, 100.11, 55.30, 22.54. HRMS (ESI<sup>+</sup>):  $m/z$  calcd for  $\text{C}_{12}\text{H}_{11}\text{N}_3\text{O}_3$  (M)<sup>+</sup> 245.0800, found 246.0802. HPLC purity 100% (230 to 400 nm).

**5-(2-(5-Methoxy-1*H*-indol-3-yl)ethyl)-1,3,4-oxadiazol-2(3*H*)-one (19).** Starting from **14** (146 mg, 0.62 mmol) and following the procedure described for **18**, oxadiazolone **19** (138 mg, 86%) was obtained as an off-white solid of mp 140 – 144 °C.  $^1\text{H}$  NMR (400 MHz, DMSO)  $\delta$  12.00 (s, 1H), 10.66 (s, 1H), 7.20 (d,  $J$  = 8.7 Hz, 1H), 7.09 (d,  $J$  = 2.3 Hz, 1H), 6.95 (d,  $J$  = 2.4 Hz, 1H), 6.69 (dd,  $J$  = 8.7, 2.4 Hz, 1H), 3.74 (s, 3H), 2.97 (t,  $J$  = 7.6 Hz, 2H), 2.85 (t,  $J$  = 7.6 Hz, 2H).  $^{13}\text{C}$  NMR (101 MHz, DMSO)  $\delta$  157.65, 155.77, 153.70, 131.92, 127.77, 124.00, 112.76, 112.72, 111.93, 100.36, 55.92, 27.55, 21.54. HRMS (ESI<sup>+</sup>):  $m/z$  calcd for  $\text{C}_{13}\text{H}_{13}\text{N}_3\text{O}_3$  (M)<sup>+</sup> 259.0957, found 259.0966. HPLC purity 100% (230 to 400 nm).

**5-((5-Methoxy-1*H*-indol-3-yl)methyl)-1,3,4-oxadiazole-2(3*H*)-thione (20).** A mixture of **13** (83 mg, 0.37 mmol), KOH (70 mg, 1.24 mmol) and an excess of carbon disulfide (1.35 mL, 38 mmol) in EtOH was heated to 155 °C for 10 min under microwave irradiation. Solvent and carbon disulfide excess were evaporated under reduced pressure and the residue treated with water. The solution was acidified with conc. HCl and **20** (91 mg, 95%) precipitated as a yellow solid of mp 171 – 173 °C that was filtered off.  $^1\text{H}$  NMR (300 MHz, DMSO)  $\delta$  14.35 (s, 1H), 10.94 (s, 1H), 7.30 (s, 1H), 7.28 (d,  $J$  = 8.8 Hz, 1H), 7.02 (d,  $J$  = 2.3 Hz, 1H), 6.76 (dd,  $J$  = 8.8, 2.4 Hz, 1H), 4.19 (s, 2H), 3.75 (s, 3H).  $^{13}\text{C}$  NMR (75 MHz, DMSO)  $\delta$  177.73, 163.44, 153.25, 131.23, 126.94, 125.01, 112.28, 111.38, 105.39, 100.08, 55.31, 21.74. HRMS (ESI<sup>+</sup>):  $m/z$  calcd for  $\text{C}_{12}\text{H}_{11}\text{N}_3\text{O}_2\text{S}$  (M)<sup>+</sup> 261.0572, found 261.0577. HPLC purity 100% (230 to 400 nm).

**5-(2-(5-Methoxy-1*H*-indol-3-yl)ethyl)-1,3,4-oxadiazole-2(3*H*)-thione (21).** Starting from **14** (116 mg, 0.5 mmol) and following the procedure described for **20**, derivative **21** (56 mg, 41%) was obtained as an off-white solid of mp 99 – 101 °C. <sup>1</sup>H NMR (400 MHz, DMSO) δ 14.29 (s, 1H), 10.70 (s, 1H), 7.21 (d, *J* = 8.7 Hz, 1H), 7.11 (d, *J* = 2.4 Hz, 1H), 6.97 (d, *J* = 2.4 Hz, 1H), 6.70 (dd, *J* = 8.7, 2.4 Hz, 1H), 3.76 (s, 3H), 3.10 – 2.97 (m, 4H). <sup>13</sup>C NMR (101 MHz, DMSO) δ 177.69, 164.05, 153.08, 131.25, 127.06, 123.38, 112.12, 111.84, 111.37, 99.70, 55.31, 26.14, 21.05. HRMS (ESI<sup>+</sup>): *m/z* calcd for C<sub>13</sub>H<sub>13</sub>N<sub>3</sub>O<sub>2</sub>S (M)<sup>+</sup> 275.0728, found 275.0726. HPLC purity 95% (230 to 400 nm).

**General Method for the Synthesis of Acyl(thio)semicarbazides.** To a solution of a hydrazide (1 mmol) in EtOH (10 mL) the corresponding isocyanate or isothiocyanate (1 mmol) was added. The mixture was kept stirring at rt until the reaction was finished, typically 1 h in the case of methylisocyanate. Longer times were needed in the case of ethylisothiocyanate. Then, solvent was removed and the resulting solid used as such for the next step without further purification.

**1-(2-(5-Methoxy-1*H*-indol-3-yl)acetyl)-4-methylsemicarbazide (22).** According to the general method, from **13** (73 mg, 0.33 mmol) and methylisocyanate (21 μL, 0.33 mmol) and after 1 h stirring at rt, intermediate **22** (91 mg, 99%) was obtained as a white solid. HPLC-MS (230 to 400 nm) 97% (*m/z*) [MH<sup>+</sup>] 277.37.

**1-(3-(5-Methoxy-1*H*-indol-3-yl)propanoyl)-4-methylsemicarbazide (23).** Following the general method, the 1h-stirring of **14** (230 mg, 0.98 mmol) and methylisocyanate (68 μL, 1 mmol) yielded intermediate **23** (290 mg, 100%) as a white solid. HPLC-MS (230 to 400 nm) 98% (*m/z*) [MH<sup>+</sup>] 291.40.

**1-(2-(5-Methoxy-1*H*-indol-3-yl)acetyl)-4-ethylthiosemicarbazide (24).** According to the general method, the 18h-stirring at rt of **13** (116 mg, 0.5 mmol) and

ethylisothiocyanate (44  $\mu$ L, 0.5 mmol) gave intermediate **24** (150 mg, 94%) as a white solid. HPLC-MS (230 to 400 nm) 99% (m/z) [MH<sup>+</sup>] 307.37.

**1-(3-(5-Methoxy-1*H*-indol-3-yl)propanoyl)-4-ethylthiosemicarbazide (25).**

According to the general method, from **14** (506 mg, 2.17 mmol) and ethylisothiocyanate (190  $\mu$ L, 2.17 mmol), using 18h of reaction at rt, intermediate **25** (707 mg, 100%) was obtained as a white solid. HPLC-MS (230 to 400 nm) 90% (m/z) [MH<sup>+</sup>] 321.26.

**General Method for the Synthesis of 1,2,4-Triazol-5-(thi)ones.** The corresponding acylsemicarbazide or acylthiosemicarbazide (1 mmol) was dissolved in EtOH (10 mL) and NaOH 2M (7 mL) was added. The mixture was heated under microwave irradiation at 100 °C for 15 min. The solvent was evaporated and the crude dissolved in water. The mixture was acidified to pH 2 with conc. HCl and the corresponding triazole precipitated off the solution, being collected by filtration. When necessary, the precipitate was chromatographed in silica gel (gradient DCM:MeOH) for further purification.

**3-((5-Methoxy-1*H*-indol-3-yl)methyl)-4-methyl-1*H*-1,2,4-triazol-5(4*H*)-one (26).**

According to the above general method, from **22** (82 mg, 0.3 mmol), triazole **26** (58 mg, 75%) was obtained as a light orange pearly solid of mp 218 – 219 °C. <sup>1</sup>H NMR (300 MHz, DMSO)  $\delta$  11.41 (s, 1H), 10.82 (s, 1H), 7.25 (d, *J* = 8.8 Hz, 1H), 7.20 (d, *J* = 2.3 Hz, 1H), 7.01 (d, *J* = 2.4 Hz, 1H), 6.74 (dd, *J* = 8.8, 2.4 Hz, 1H), 3.95 (s, 2H), 3.72 (s, 3H), 2.98 (s, 3H). <sup>13</sup>C NMR (75 MHz, DMSO)  $\delta$  155.65, 153.43, 147.20, 131.77, 127.50, 124.77, 112.51, 111.55, 107.40, 100.68, 55.65, 26.88, 22.86. HRMS (ESI<sup>+</sup>): *m/z* calcd for C<sub>13</sub>H<sub>14</sub>N<sub>4</sub>O<sub>2</sub> (M)<sup>+</sup> 258.1117, found 258.1113. HPLC purity 100% (230 to 400 nm).

**3-(2-(5-Methoxy-1*H*-indol-3-yl)ethyl)-4-methyl-1*H*-1,2,4-triazol-5(4*H*)-one (27).**

Following the general method, from **23** (290 mg, 1 mmol) and after a chromatographic purification on silica gel, **27** (110 mg, 41%) was obtained as a white powder of mp 201 – 202 °C. <sup>1</sup>H NMR (500 MHz, DMSO) δ 11.38 (s, 1H), 10.67 (s, 1H), 7.22 (d, *J* = 8.8 Hz, 1H), 7.12 (d, *J* = 2.4 Hz, 1H), 6.94 (d, *J* = 2.4 Hz, 1H), 6.70 (dd, *J* = 8.8, 2.4 Hz, 1H), 3.75 (s, 3H), 3.01 (s, 3H), 2.98 (t, *J* = 8.0 Hz, 2H), 2.82 (t, *J* = 8.0 Hz, 2H). <sup>13</sup>C NMR (126 MHz, DMSO) δ 155.65, 153.39, 148.13, 131.70, 127.66, 123.70, 113.24, 112.45, 111.60, 100.26, 55.68, 26.75, 26.74, 21.74. HRMS (ESI<sup>+</sup>): Calcd. for C<sub>14</sub>H<sub>16</sub>N<sub>4</sub>O<sub>2</sub> (M)<sup>+</sup> 272.1283, found *m/z* 272.1273. HPLC purity 100% (230 to 400 nm).

**4-Ethyl-3-((5-methoxy-1*H*-indol-3-yl)methyl)-1*H*-1,2,4-triazol-5(4*H*)-thione (28).**

According to the general method, from **24** (40 mg, 0.13 mmol), triazole **28** (30 mg, 80%) was obtained as a shiny brownish solid of mp: 200 - 203 °C. <sup>1</sup>H NMR (300 MHz, DMSO) δ 13.51 (s, 1H), 10.87 (s, 1H), 7.27 (d, *J* = 2.5 Hz, 1H), 7.25 (d, *J* = 8.8 Hz, 1H), 6.98 (d, *J* = 2.4 Hz, 1H), 6.74 (dd, *J* = 8.8, 2.4 Hz, 1H), 4.16 (s, 2H), 3.90 (q, *J* = 7.1 Hz, 2H), 3.72 (s, 3H), 0.93 (t, *J* = 7.1 Hz, 3H). <sup>13</sup>C NMR (75 MHz, DMSO) δ 166.63, 153.49, 151.61, 131.74, 127.43, 125.08, 112.60, 111.58, 107.29, 100.65, 55.65, 38.62, 22.22, 13.23. HRMS (ESI<sup>+</sup>): *m/z* calcd for C<sub>14</sub>H<sub>16</sub>N<sub>4</sub>OS (M)<sup>+</sup> 288.1045, found 288.1036. HPLC purity 100% (230 to 400 nm).

**4-Ethyl-3-(2-(5-methoxy-1*H*-indol-3-yl)ethyl)-1*H*-1,2,4-triazol-5(4*H*)-thione (29).**

Following the general method, from **25** (200 mg, 0.62 mmol), and after chromatographic purification on silica gel, **29** (140 mg, 84%) was obtained as a white powder of mp 214 – 217 °C. <sup>1</sup>H NMR (500 MHz, DMSO) δ 13.52 (s, 1H), 10.68 (s, 1H), 7.22 (d, *J* = 8.7 Hz, 1H), 7.14 (d, *J* = 2.4 Hz, 1H), 6.96 (d, *J* = 2.4 Hz, 1H), 6.70 (dd, *J* = 8.7, 2.4 Hz, 1H), 3.91 (q, *J* = 7.2 Hz, 2H), 3.75 (s, 3H), 3.06 – 3.02 (m, 2H), 3.02 – 2.97 (m, 2H), 1.14 (t, *J* = 7.2 Hz, 3H). <sup>13</sup>C NMR (126 MHz, DMSO) δ 166.26,

153.42, 152.45, 131.69, 127.60, 123.77, 113.04, 112.48, 111.66, 100.24, 55.69, 38.40, 26.15, 22.05, 13.77. HRMS (ESI<sup>+</sup>): Calcd for C<sub>15</sub>H<sub>18</sub>N<sub>4</sub>OS (M)<sup>+</sup> 302.1201, found *m/z* 302.1207. HPLC-MS (230 to 400 nm) 98% (*m/z*) (M<sup>+</sup>) 303.28.

***N*-Ethyl-5-((5-methoxy-1*H*-indol-3-yl)methyl)-1,3,4-thiadiazol-2-amine (30).**

POCl<sub>3</sub> (1 mL) was added over intermediate **24** (92 mg, 0.3 mmol) and the mixture kept stirring at rt for 18 h. After this time, water (10 mL) was carefully added to the mixture and then basified at 0 °C to pH 9-10 with NaOH 2M. The mixture was extracted with EtOAc (3 x 20 mL), and the extracts dried over MgSO<sub>4</sub>. After evaporation of the solvent **30** (58 mg, 67%) was isolated as an off-white solid of mp 136 – 139 °C. <sup>1</sup>H NMR (500 MHz, DMSO) δ 10.78 (s, 1H), 7.40 (t, *J* = 5.3 Hz, 1H), 7.23 (d, *J* = 8.7 Hz, 1H), 7.21 (d, *J* = 2.5 Hz, 1H), 6.94 (d, *J* = 2.4 Hz, 1H), 6.72 (dd, *J* = 8.7, 2.4 Hz, 1H), 4.19 (s, 2H), 3.70 (s, 3H), 3.18 (qd, *J* = 7.2, 5.3 Hz, 2H), 1.09 (t, *J* = 7.2 Hz, 3H). <sup>13</sup>C NMR (126 MHz, DMSO) δ 168.98, 159.10, 153.54, 131.84, 127.39, 124.74, 112.63, 111.64, 110.96, 100.72, 55.76, 39.63, 26.47, 14.74. HRMS (ESI<sup>+</sup>): Calcd. for C<sub>14</sub>H<sub>16</sub>N<sub>4</sub>OS (M)<sup>+</sup> 288.1045, found *m/z* 288.1050. HPLC-MS (230 to 400 nm) 95% (*m/z*) [MH<sup>+</sup>] 289.40.

**Pharmacology. Assays for human MT<sub>1</sub>R and MT<sub>2</sub>R subtypes.** 2-[<sup>125</sup>I]Iodomelatonin (2200 Ci/mmol) was purchased from NEN (Boston, MA). Other drugs and chemicals were purchased from Sigma–Aldrich (Saint Quentin, France).

2-[<sup>125</sup>I]Iodomelatonin binding assay conditions were essentially as previously described.<sup>85</sup> Briefly, binding was initiated by addition of membrane preparations from transfected CHO cells stably expressing the human MT<sub>1</sub>R or MT<sub>2</sub>R diluted in binding buffer (50 mM Tris–HCl buffer, pH 7.4, containing 5 mM MgCl<sub>2</sub>) to 2-[<sup>125</sup>I]iodomelatonin (20 pM) and the tested drug. Non-specific binding was defined in

the presence of 1  $\mu$ M melatonin. After 120 min incubation at 37  $^{\circ}$ C, reaction was stopped by rapid filtration through GF/B filters presoaked in 0.5% (v/v) polyethylenimine. Filters were washed three times with 1 mL of ice-cold 50 mM Tris–HCl buffer, pH 7.4.

Data from the dose-response curves (seven concentrations in duplicate) were analysed using the program PRISM (Graph Pad Software Inc., San Diego, CA) to yield  $IC_{50}$  (inhibitory concentration 50) values. Results are expressed as  $K_i = IC_{50} / (1 + ([L]/K_D))$ , where [L] is the concentration of radioligand used in the assay and  $K_D$  the dissociation constant of the radioligand characterizing the membrane preparation.

$[^{35}\text{S}]\text{GTP}\gamma\text{S}$  binding assay was performed according to published methodology.<sup>85</sup> Briefly, membranes from transfected CHO cells expressing  $MT_1R$  or  $MT_2R$  subtypes and compounds were diluted in binding buffer (20 mM HEPES, pH 7.4, 100 mM NaCl, 3  $\mu$ M GDP, 3 mM  $\text{MgCl}_2$ , and 20  $\mu$ g/mL saponin). Incubation was started by the addition of 0.2 nM  $[^{35}\text{S}]\text{GTP}\gamma\text{S}$  to membranes (20  $\mu$ g/mL) and drugs, and further followed for 1 h at rt. Reaction was stopped by rapid filtration through GF/B filters followed by three successive washes with ice-cold buffer.

Usual levels of  $[^{35}\text{S}]\text{GTP}\gamma\text{S}$  binding (expressed in dpm) were for CHO- $MT_2$  membranes: 2000 for basal activity, 8000 in the presence of melatonin 1  $\mu$ M and 180 in the presence of  $\text{GTP}\gamma\text{S}$  10  $\mu$ M which defined the non-specific binding. Data from the dose-response curves (seven concentrations in duplicate) were analyzed by using the program PRISM (Graph Pad Software Inc., San Diego, CA) to yield  $EC_{50}$  (the effective concentration 50%) and  $E_{\text{max}}$  (maximal effect) for agonists.

***In vitro* Blood–Brain Barrier Permeation Assay (PAMPA).** Prediction of the brain penetration was performed using a parallel artificial membrane permeation assay (PAMPA-BBB), in a similar manner as previously described.<sup>43,56,57</sup> Pipetting was done

with a semi-automatic pipettor (CyBi<sup>®</sup>-SELMA) and UV reading with a microplate spectrophotometer (Multiskan Spectrum, Thermo Electron Co.). Commercial drugs, phosphate buffered saline solution at pH 7.4 (PBS), and dodecane were purchased from Sigma, Aldrich, Acros, and Fluka. Millex filter units (PVDF membrane, diameter 25 mm, pore size 0.45  $\mu\text{m}$ ) were acquired from Millipore. The porcine brain lipid (PBL) was obtained from Avanti Polar Lipids. The donor microplate was a 96-well filter plate (PVDF membrane, pore size 0.45  $\mu\text{m}$ ) and the acceptor microplate was an indented 96-well plate, both from Millipore. The acceptor 96-well microplate was filled with 200  $\mu\text{L}$  of PBS:ethanol (70:30) and the filter surface of the donor microplate was impregnated with 4  $\mu\text{L}$  of porcine brain lipid (PBL) in dodecane (20  $\text{mg mL}^{-1}$ ). Compounds were dissolved in PBS:ethanol (70:30) at 100  $\mu\text{g mL}^{-1}$ , filtered through a Millex filter, and then added to the donor wells (200  $\mu\text{L}$ ). The donor filter plate was carefully put on the acceptor plate to form a sandwich, which was left undisturbed for 240 min at 25  $^{\circ}\text{C}$ . After incubation, the donor plate was carefully removed and the concentration of compounds in the acceptor wells was determined by UV-Vis spectroscopy. Every sample was analyzed at five wavelengths, in four wells and at least in three independent runs, and the results are given as the mean  $\pm$  standard deviation. In each experiment, 11 quality control standards of known BBB permeability were included to validate the analysis set.

**Thermodynamic solubility determination.** The solubility experiments were performed following in part described protocols.<sup>51,52</sup> UV maximums are extracted from recorded UV-spectra of the compounds in the 270-400 nm range. A 10 mM stock solution of each compound in DMSO is prepared. A calibration line is built by measuring the absorbance at the corresponding maximum wavelength of sequential dilutions of the stock solution in buffer-MeCN (80:20) mixture in a 96-well plate containing 200  $\mu\text{L}$  per

point. The buffers employed are: pH 1.2 KCl 45 mM buffer, pH 7.4 phosphate 45 mM buffer and pH 9.4 NH<sub>4</sub>Cl buffer. In order to validate the calibration line, and exclude interferences due to the presence of 5% DMSO, a quality control standard of known solubility is employed. The calibration line is accepted if  $R^2 > 0.990$ , the residual value of each point  $< 15\%$  and the relative error of the quality control standard  $< 15\%$ . The solubility determination is made as follows: 200  $\mu$ L of buffer solution are added over approximately 1 mg accurately weighted of the tested compound in order to achieve a saturated solution. The mixture is kept at rt in an orbital stirrer at 320 rpm for 24 h and then centrifuged at 135 rpm for 15 min. 160  $\mu$ L of the supernatant are transferred to a 96-well plate and diluted with 40  $\mu$ L of a buffer-MeCN (80:20) mixture. The solubility is calculated by extrapolation to the calibration line within the linearity range and expressed in mol/L. The experiments were run in triplicates.

**Molecular superposition.** Compounds were built with Maestro 9.2<sup>86</sup> and subjected to an energy minimization procedure using the OPLS2005 force field<sup>87</sup> to a convergence threshold of 0.05 kJ mol<sup>-1</sup> Å<sup>-1</sup>. Compounds were superposed to the putative bioactive conformation of melatonin,<sup>6</sup> having torsion angles:  $\tau_1$  (C3a–C3–C $\beta$ –C $\alpha$ )  $\approx -78^\circ$ ;  $\tau_2$  (C3–C $\beta$ –C $\alpha$ –N)  $\approx 180^\circ$ ;  $\tau_3$  (C $\beta$ –C $\alpha$ –N–CO)  $\approx -177^\circ$ . Superposed atoms are: the methoxy oxygen, C3a, C5 and C7 of the benzene ring of indoles, and the amide oxygen of melatonin that was superposed to the N atom within the five-membered cycles.

**Neurogenesis Assays.** *Animals.* Adult (8-12 weeks old) male Wistar rats (n = 6 per group), housed in a 12 h light-dark cycle animal facility, were used in this study. All procedures with animals were specifically approved by the Ethics Committee for Animal Experimentation of the CSIC and carried out in accordance with National (normative 1201/2005) and International recommendations (Directive 2010/63 from the European Communities Council). Special care was taken to minimize animal suffering.



1  
2  
3 *Neurosphere cultures.* NS were derived from the SGZ of the dentate gyrus of the  
4 hippocampus of adult Wistar rats, and induced to proliferate using established passaging  
5 methods to achieve optimal cellular expansion according to published protocols.<sup>54</sup> Rats  
6 were decapitated and brains dissected, obtaining the SVZ and the hippocampus as  
7 described.<sup>55</sup> Briefly, cells were seeded into 12-well dishes and cultured in Dubecco's  
8 Modified Eagle's Medium (DMEM)/F12 (1:1, Invitrogen) containing 10 ng/mL  
9 epidermal growth factor (EGF, Peprotech, London, UK), 10 ng/mL fibroblast growth  
10 factor (FGF, Peprotech), and B27 medium (Gibco). After 3 days in culture, primary NS  
11 cultures were treated with different compounds for 7 days. To determine the ability of  
12 compounds to induce differentiation, then NS were plated onto 100 µg/mL poly-L-  
13 lysine-coated coverslips and treated for 48 h in the presence of serum, but in absence of  
14 exogenous growth factors.<sup>88</sup>

15  
16  
17  
18  
19  
20  
21  
22  
23  
24  
25  
26  
27  
28  
29 *Immunocytochemistry.* After treatment, cells were processed for  
30 immunocytochemistry with two types of neurogenesis-associated neuronal markers:  
31 TuJ1, associated with early stages of neurogenesis, and MAP-2, a marker of neuronal  
32 maturation. DAPI staining was used as a nuclear marker. Basal values were obtained  
33 under the same conditions, but in the absence of any product. Melatonin (endogenous  
34 ligand of the MTRs) and luzindole (melatonergic antagonist) were used as controls. The  
35 images were obtained using a Nikon fluorescence microscope 90i that was coupled to a  
36 digital camera Qi. The microscope configuration was adjusted to produce the optimum  
37 signal-to-noise ratio. The number of TuJ-1 and MAP-2 expressing cells in the NS was  
38 estimated as previously described.<sup>88</sup> Cell numbers were estimated from a total of five  
39 NS per condition over three independent experiments.

40  
41  
42  
43  
44  
45  
46  
47  
48  
49  
50  
51  
52  
53  
54  
55  
56  
57  
58  
59  
60

*Statistical analysis.* The SPSS statistical software package (version 20.0) for Windows (Chicago, IL) was used for the ANOVA (one-way) analyses followed by Student's t post hoc test. A p value  $\leq 0.05$  was considered to be statistically significant.

## ASSOCIATED CONTENT

### Supporting Information

NMR studies on the tautomerism of hydrogen-bearing azoles **18** and **30**. This material is available free of charge via the Internet at <http://pubs.acs.org>.

## AUTHOR INFORMATION

### Corresponding Author

\*Mailing address: Dr. María Isabel Rodríguez-Franco, Instituto de Química Médica (IQM-CSIC), C/ Juan de la Cierva 3, 28006 Madrid (Spain). Phone: 34-91-5622900. Fax: 34-91-5644853. E-mail: [isabelrguez@iqm.csic.es](mailto:isabelrguez@iqm.csic.es)

### Note

The authors declare no competing financial interest.

## ACKNOWLEDGMENTS

We gratefully acknowledge the financial support of the Spanish Ministry of Economy and Competitiveness (MINECO, grants SAF2012-31035 and SAF2010-16365), Fundación de Investigación Médica Mutua Madrileña Automovilística (grant AP103952012), and Consejo Superior de Investigaciones Científicas (CSIC, grant PIE-201280E074). The Centro de Investigación Biomédica en Red sobre Enfermedades Neurodegenerativas (CIBERNED) is funded by the Instituto de Salud Carlos III. M.F.R. thanks CSIC for a JAE-Predocctoral Contract and J.A.M.-G. thanks the Postdoctoral Fellowship from CIBERNED. We also acknowledge Dr. Paula Morales for the binding

assays on cannabinoid receptors and the National Institute on Mental Health-Psychoactive Drug Screening Program (NIMH-PDSP, Contract #HHSN-271-2013-00017-C, Dr. Bryan Roth) for binding experiments on serotonin receptors and transporter.

#### ABBREVIATIONS USED

BBB, blood-brain barrier; CDI, carbonyldiimidazole; CHO, Chinese hamster ovary; COSY, homonuclear correlation spectroscopy; DAPI, 4',6-diamidino-2-phenylindole; DMAP, dimethylaminopyridine; EC<sub>50</sub>, half maximal effective concentration;  $E_{\max}$ , maximal effect; GPCRs, G-protein-coupled receptors; GTP $\gamma$ S, guanosine 5'-O-(3-thiotriphosphate); HMBC, heteronuclear multiple bond correlation; HRMS, high resolution mass spectrum; HSQC, heteronuclear single quantum coherence;  $K_i$ , binding constant; MAP-2, microtubule-associated protein 2; 5-MeO-DMT, 5-methoxy-*N,N*-dimethyl-tryptamine; MTRs, melatonin receptors; MT<sub>1</sub>R: melatonin receptor subtype 1; MT<sub>2</sub>R: melatonin receptor subtype 2; NMR, nuclear magnetic resonance; NS, neurospheres; SEM, standard error of the mean; SGZ, subgranular zone; SVZ, subventricular zone; TEA, triethylamine; THF, tetrahydrofuran; TuJ1,  $\beta$ -tubulin III marker

## REFERENCES

- (1) Hardeland, R.; Cardinali, D. P.; Srinivasan, V.; Spence, D. W.; Brown, G. M.; Pandi-Perumal, S. R. Melatonin--a pleiotropic, orchestrating regulator molecule. *Prog. Neurobiol.* **2011**, *93*, 350-384.
- (2) Zlotos, D. P.; Jockers, R.; Cecon, E.; Rivara, S.; Witt-Enderby, P. A. MT<sub>1</sub> and MT<sub>2</sub> melatonin receptors: ligands, models, oligomers, and therapeutic potential. *J. Med. Chem.* **2014**, *57*, 3161-3185.
- (3) Pala, D.; Lodola, A.; Bedini, A.; Spadoni, G.; Rivara, S. Homology models of melatonin receptors: challenges and recent advances. *Int. J. Mol. Sci.* **2013**, *14*, 8093-8121.
- (4) Mor, M.; Rivara, S.; Pala, D.; Bedini, A.; Spadoni, G.; Tarzia, G. Recent advances in the development of melatonin MT(1) and MT(2) receptor agonists. *Expert Opin. Ther. Pat.* **2010**, *20*, 1059-1077.
- (5) Pala, D.; Beuming, T.; Sherman, W.; Lodola, A.; Rivara, S.; Mor, M. Structure-based virtual screening of MT<sub>2</sub> melatonin receptor: influence of template choice and structural refinement. *J. Chem. Inf. Model.* **2013**, *53*, 821-835.
- (6) Rivara, S.; Diamantini, G.; Di Giacomo, B.; Lamba, D.; Gatti, G.; Lucini, V.; Pannacci, M.; Mor, M.; Spadoni, G.; Tarzia, G. Reassessing the melatonin pharmacophore—Enantiomeric resolution, pharmacological activity, structure analysis, and molecular modeling of a constrained chiral melatonin analogue. *Bioorg. Med. Chem.* **2006**, *14*, 3383-3391.
- (7) Jansen, J. M.; Copping, S.; Gruppen, G.; Molinari, E. J.; Dubocovich, M. L.; Grol, C. J. The high affinity melatonin binding site probed with conformationally restricted ligands—I. Pharmacophore and minireceptor models. *Bioorg Med. Chem.* **1996**, *4*, 1321-1332.

- (8) Depreux, P.; Lesieur, D.; Mansour, H. A.; Morgan, P. r.; Howell, H. E.; Renard, P.; Caignard, D.-H.; Pfeiffer, B.; Delagrange, P. Synthesis and structure-activity relationships of novel naphthalenic and bioisosteric related amidic derivatives as melatonin receptor ligands. *J. Med. Chem.* **1994**, *37*, 3231-3239.
- (9) Uchikawa, O.; Fukatsu, K.; Tokunoh, R.; Kawada, M.; Matsumoto, K.; Imai, Y.; Hinuma, S.; Kato, K.; Nishikawa, H.; Hirai, K.; Miyamoto, M.; Ohkawa, S. Synthesis of a novel series of tricyclic indan derivatives as melatonin receptor agonists. *J. Med. Chem.* **2002**, *45*, 4222-4239.
- (10) Tsotinis, A.; Afroudakis, P. A.; Garratt, P. J.; Bocianowska-Zbrog, A.; Sugden, D. Benzocyclobutane, benzocycloheptane and heptene derivatives as melatonin agonists and antagonists. *ChemMedChem* **2014**, *9*, 2238-2243.
- (11) Rivara, S.; Lorenzi, S.; Mor, M.; Plazzi, P. V.; Spadoni, G.; Bedini, A.; Tarzia, G. Analysis of structure-activity relationships for MT<sub>2</sub> selective antagonists by melatonin MT<sub>1</sub> and MT<sub>2</sub> receptor models. *J. Med. Chem.* **2005**, *48*, 4049-4060.
- (12) Dubocovich, M. L. Luzindole (N-0774): a novel melatonin receptor antagonist. *J. Pharmacol. Exp. Ther.* **1988**, *246*, 902-910.
- (13) Laudon, M.; Zisapel, N. Characterization of central melatonin receptors using <sup>125</sup>I-melatonin. *FEBS Lett.* **1986**, *197*, 9-12.
- (14) Vakkuri, O.; Lämsä, E.; Rahkamaa, E.; Ruotsalainen, H.; Leppäluoto, J. Iodinated melatonin: preparation and characterization of the molecular structure by mass and <sup>1</sup>H NMR spectroscopy. *Anal. Biochem.* **1984**, *142*, 284-289.
- (15) Waring, M. J. Lipophilicity in drug discovery. *Expert Opin. Drug Discovery* **2010**, *5*, 235-248.

- (16) Ritchie, T. J.; Macdonald, S. J. F. The impact of aromatic ring count on compound developability – are too many aromatic rings a liability in drug design? *Drug Discovery Today* **2009**, *14*, 1011-1020.
- (17) Arnott, J. A.; Planey, S. L. The influence of lipophilicity in drug discovery and design. *Expert Opin. Drug Discovery* **2012**, *7*, 863-875.
- (18) Bissantz, C.; Kuhn, B.; Stahl, M. A medicinal chemist's guide to molecular interactions. *J. Med. Chem.* **2010**, *53*, 5061-5084.
- (19) Leclerc, V.; Fourmaintraux, E.; Depreux, P.; Lesieur, D.; Morgan, P.; Howell, H. E.; Renard, P.; Caignard, D. H.; Pfeiffer, B.; Delagrange, P.; Guardiola-Lemaître, B.; Andrieux, J. Synthesis and structure-activity relationships of novel naphthalenic and bioisosteric related amidic derivatives as melatonin receptor ligands. *Bioorg. Med. Chem.* **1998**, *6*, 1875-1887.
- (20) Willis, G. L. The role of ML-23 and other melatonin analogues in the treatment and management of Parkinson's disease. *Drug News Perspect.* **2005**, *18*, 437-444.
- (21) Morgan, P. J.; Williams, L. M.; Davidson, G.; Lawson, W.; Howell, E. Melatonin receptors on ovine pars tuberalis: characterization and autoradiographic localization. *J. Neuroendocrinol.* **1989**, *1*, 1-4.
- (22) Laudon, M.; Peleg-Shulgman, T. Pyrone-indole derivatives and process for their preparation. US 7,635,710 B2 (2009).
- (23) He, P.; Ouyang, X.; Zhou, S.; Yin, W.; Tang, C.; Laudon, M.; Tian, S. A novel melatonin agonist Neu-P11 facilitates memory performance and improves cognitive impairment in a rat model of Alzheimer' disease. *Horm. Behav.* **2013**, *64*, 1-7.
- (24) Tian, S.-W.; Laudon, M.; Han, L.; Gao, J.; Huang, F.-L.; Yang, Y.-F.; Deng, H.-F. Antidepressant- and anxiolytic effects of the novel melatonin agonist Neu-P11 in rodent models. *Acta Pharmacol. Sin.* **2010**, *31*, 775-783.

- (25) Rami, M.; Landagaray, E.; Ettaoussi, M.; Boukhalfa, K.; Caignard, D.-H.; Delagrangé, P.; Berthelot, P.; Yous, S. Novel conformationally constrained analogues of agomelatine as new melatoninergic ligands. *Molecules* **2012**, *18*, 154-166.
- (26) Boström, J.; Hogner, A.; Llinàs, A.; Wellner, E.; Plowright, A. T. Oxadiazoles in medicinal chemistry. *J. Med. Chem.* **2011**, *55*, 1817-1830.
- (27) Shen, H.-W.; Jiang, X.-L.; Winter, J. C.; Yu, A.-M. Psychedelic 5-methoxy-*N,N*-dimethyltryptamine: metabolism, pharmacokinetics, drug interactions, and pharmacological actions. *Curr. Drug Metab.* **2010**, *11*, 659-666.
- (28) Duncan, M. J.; Takahashi, J. S.; Dubocovich, M. L. 2-[<sup>125</sup>I]Iodomelatonin binding sites in hamster brain membranes: pharmacological characteristics and regional distribution. *Endocrinology* **1988**, *122*, 1825-1833.
- (29) Basarab, G. S.; Manchester, J. I.; Bist, S.; Boriack-Sjodin, P. A.; Dangel, B.; Illingworth, R.; Sherer, B. A.; Sriram, S.; Uria-Nickelsen, M.; Eakin, A. E. Fragment-to-hit-to-lead discovery of a novel pyridylurea scaffold of ATP competitive dual targeting type II topoisomerase inhibiting antibacterial agents. *J. Med. Chem.* **2002**, *56*, 8712-8735.
- (30) Ramírez-Rodríguez, G.; Klempin, F.; Babu, H.; Benítez-King, G.; Kempermann, G. Melatonin modulates cell survival of new neurons in the hippocampus of adult mice. *Neuropsychopharmacology* **2009**, *34*, 2180-2191.
- (31) Kempermann, G.; Jessberger, S.; Steiner, B.; Kronenberg, G. Milestones of neuronal development in the adult hippocampus. *Trends Neurosci.* **2004**, *27*, 447-452.
- (32) Mongiat, L. A.; Schinder, A. F. Neuroscience. A price to pay for adult neurogenesis. *Science* **2014**, *344*, 594-595.
- (33) Duman, R. S.; Malberg, J.; Nakagawa, S. Regulation of adult neurogenesis by psychotropic drugs and stress. *J. Pharmacol. Exp. Ther.* **2001**, *299*, 401-407.

- (34) Rolando, C.; Taylor, V. Neural stem cell of the hippocampus: development, physiology regulation, and dysfunction in disease. *Curr. Top. Dev. Biol.* **2014**, *107*, 183-206.
- (35) Abdipranoto, A.; Wu, S.; Stayte, S.; Vissel, B. The role of neurogenesis in neurodegenerative diseases and its implications for therapeutic development. *CNS Neurol. Disord. Drug Targets* **2008**, *7*, 187-210.
- (36) Iguichi, H.; Kato, K. I.; Ibayashi, H. Age-dependent reduction in serum melatonin concentrations in healthy human subjects. *J. Clin. Endocrinol. Metab.* **1982**, *55*, 27-29.
- (37) Ramírez-Rodríguez, G.; Vega-Rivera, N. M.; Benítez-King, G.; Castro-García, M.; Ortiz-López, L. Melatonin supplementation delays the decline of adult hippocampal neurogenesis during normal aging of mice. *Neurosci. Lett.* **2012**, *530*, 53-58.
- (38) López, L. C.; Escames, G.; López, A.; García, J. A.; Doerrier, C.; Acuña-Castroviejo, D. Melatonin, neurogenesis, and aging brain. *Open Neuroendocrinol. J.* **2010**, *3*, 121-133.
- (39) Poeggeler, B. Melatonin, aging, and age-related diseases. *Endocrine* **2005**, *27*, 201-212.
- (40) Rodríguez-Franco, M. I.; Fernández-Bachiller, M. I.; Pérez, C.; Hernández-Ledesma, B.; Bartolomé, B. Novel tacrine-melatonin hybrids as dual-acting drugs for Alzheimer disease, with improved acetylcholinesterase inhibitory and antioxidant properties. *J. Med. Chem.* **2006**, *49*, 459-462.
- (41) Fernández-Bachiller, M. I.; Pérez, C.; Campillo, N. E.; Páez, J. A.; González-Muñoz, G. C.; Usán, P.; García-Palomero, E.; López, M. G.; Villarroja, M.; García, A. G.; Martínez, A.; Rodríguez-Franco, M. I. Tacrine-melatonin hybrids as multifunctional



agents for Alzheimer's disease, with cholinergic, antioxidant, and neuroprotective properties. *ChemMedChem* **2009**, *4*, 828-841.

(42) Spuch, C.; Antequera, D.; Fernández-Bachiller, M. I.; Rodríguez-Franco, M. I.; Carro, E. A new tacrine-melatonin hybrid reduces amyloid burden and behavioral deficits in a mouse model of Alzheimer's disease. *Neurotox. Res.* **2010**, *17*, 421-431.

(43) López-Iglesias, B.; Pérez, C.; Morales-García, J. A.; Alonso-Gil, S.; Pérez-Castillo, A.; Romero, A.; López, M. G.; Villarroja, M.; Conde, S.; Rodríguez-Franco, M. I. New melatonin-*N,N*-dibenzyl(*N*-methyl)amine hybrids: Potent neurogenic agents with antioxidant, cholinergic, and neuroprotective properties as innovative drugs for Alzheimer's disease. *J. Med. Chem.* **2014**, *57*, 3773-3785.

(44) de la Fuente Revenga, M.; Pérez, C.; Morales-García, J. A.; Alonso-Gil, S.; Pérez-Castillo, A.; Caignard, D. H.; Yáñez, M.; Gamo, A. M.; Rodríguez-Franco, M. I. Neurogenic potential assessment and pharmacological characterization of 6-methoxy-1,2,3,4-tetrahydro-beta-carboline (pinoline) and melatonin-pinoline hybrids. *ACS Chem. Neurosci.* **2015**, *6*, 800-810.

(45) Verniest, G.; England, D.; De Kimpe, N.; Padwa, A. Synthesis of substituted  $\beta$ -carbolines via gold(III)-catalyzed cycloisomerization of *N*-propargylamides. *Tetrahedron* **2010**, *66*, 1496-1502.

(46) Verniest, G.; Padwa, A. Gold- and silver-mediated cycloisomerizations of *N*-propargylamides. *Org. Lett.* **2008**, *10*, 4379-4382.

(47) Kumar, V.; Kaur, S.; Kumar, S.  $ZrCl_4$  catalyzed highly selective and efficient Michael addition of heterocyclic enamines with  $\alpha,\beta$ -unsaturated olefins. *Tetrahedron Lett.* **2006**, *47*, 7001-7005.

(48) Saitoh, M.; Kunitomo, J.; Kimura, E.; Iwashita, H.; Uno, Y.; Onishi, T.; Uchiyama, N.; Kawamoto, T.; Tanaka, T.; Mol, C. D.; Dougan, D. R.; Textor, G. P.;

- Snell, G. P.; Takizawa, M.; Itoh, F.; Kori, M. 2-{3-[4-(Alkylsulfinyl)phenyl]-1-benzofuran-5-yl}-5-methyl-1,3,4-oxadiazole derivatives as novel inhibitors of glycogen synthase kinase-3 $\beta$  with good brain permeability. *J. Med. Chem.* **2009**, *52*, 6270-6286.
- (49) Zoumpoulakis, P.; Camoutsis, C.; Pairas, G.; Soković, M.; Glamočlija, J.; Potamitis, C.; Pitsas, A. Synthesis of novel sulfonamide-1,2,4-triazoles, 1,3,4-thiadiazoles and 1,3,4-oxadiazoles, as potential antibacterial and antifungal agents. Biological evaluation and conformational analysis studies. *Bioorg. Med. Chem.* **2012**, *20*, 1569-1583.
- (50) Audinot, V.; Mailliet, F.; Lahaye-Brasseur, C.; Bonnaud, A.; Le Gall, A.; Amossé, C.; Dromaint, S.; Rodriguez, M.; Nagel, N.; Galizzi, J.-P.; Malpoux, B.; Guillaumet, G.; Lesieur, D. I.; Lefoulon, F.; Renard, P.; Delagrangé, P.; Boutin, J. A. New selective ligands of human cloned melatonin MT<sub>1</sub> and MT<sub>2</sub> receptors. *Naunyn-Schmiedeberg's Arch. Pharmacol.* **2003**, *367*, 553-561.
- (51) Bard, B.; Martel, S.; Carrupt, P. A. High throughput UV method for the estimation of thermodynamic solubility and the determination of the solubility in biorelevant media. *Eur. J. Pharm. Sci.* **2008**, *33*, 230-240.
- (52) Tan, H.; Semin, D.; Wacker, M.; Cheetham, J. An automated screening assay for determination of aqueous equilibrium solubility enabling SPR study during drug lead optimization. *J. Lab. Autom.* **2005**, *10*, 364-373.
- (53) Zubets, I. V.; Vergizov, S. N.; Yakovlev, S. I.; V'Yunov, K. A. Basicity and mechanism of transmission of electronic effects of substituents in the series of 2-amino-5-aryl-1,3,4-thiadiazoles. *Chem. Heterocycl. Compd.* **1987**, *23*, 225-228.
- (54) Ferrón, S. R.; Andreu-Agulló, C.; Mira, H.; Sánchez, P.; Marqués-Torrejón, M. A.; Fariñas, I. A combined *ex/in vivo* assay to detect effects of exogenously added factors in neural stem cells. *Nat. Protoc.* **2007**, *2*, 849-859.

- (55) Morales-García, J. A.; Luna-Medina, R.; Alfaro-Cervello, C.; Cortes-Canteli, M.; Santos, A.; García-Verdugo, J. M.; Pérez-Castillo, A. Peroxisome proliferator-activated receptor gamma ligands regulate neural stem cell proliferation and differentiation *in vitro* and *in vivo*. *Glia* **2011**, *59*, 293-307.
- (56) Di, L.; Kerns, E. H.; Fan, K.; McConnell, O. J.; Carter, G. T. High throughput artificial membrane permeability assay for blood–brain barrier. *Eur. J. Med. Chem.* **2003**, *38*, 223-232.
- (57) Fernández-Bachiller, M. I.; Pérez, C.; Monjas, L.; Rademann, J.; Rodríguez-Franco, M. I. New tacrine-4-oxo-4*H*-chromene hybrids as multifunctional agents for the treatment of Alzheimer's disease, with cholinergic, antioxidant, and beta-amyloid-reducing properties. *J. Med. Chem.* **2012**, *55*, 1303-1317.
- (58) Conway, S.; Canning, S. J.; Howell, H. E.; Mowat, E. S.; Barrett, P.; Drew, J. E.; Delagrangé, P.; Lesieur, D.; Morgan, P. J. Characterisation of human melatonin MT<sub>1</sub> and MT<sub>2</sub> receptors by CRE-luciferase reporter assay. *Eur. J. Pharmacol.* **2000**, *390*, 15-24.
- (59) Bedini, A.; Lucarini, S.; Spadoni, G.; Tarzia, G.; Scaglione, F.; Dugnani, S.; Pannacci, M.; Lucini, V.; Carmi, C.; Pala, D.; Rivara, S.; Mor, M. Toward the definition of stereochemical requirements for MT<sub>2</sub>-selective antagonists and partial agonists by studying 4-phenyl-2-propionamidotetralin derivatives. *J. Med. Chem.* **2011**, *54*, 8362-8372.
- (60) Mattson, R. J.; Catt, J. D.; Keavy, D.; Sloan, C. P.; Epperson, J.; Gao, Q.; Hodges, D. B.; Iben, L.; Mahle, C. D.; Ryan, E.; Yocca, F. D. Indanyl piperazines as melatonergic MT<sub>2</sub> selective agents. *Bioorg. Med. Chem. Lett.* **2003**, *13*, 1199-1202.
- (61) Durieux, S.; Chanu, A.; Bochu, C.; Audinot, V.; Coumailleau, S.; Boutin, J. A.; Delagrangé, P.; Caignard, D.-H.; Bennejean, C.; Renard, P.; Lesieur, D.; Berthelot, P.;

- Yous, S. Design and synthesis of 3-phenyltetrahydronaphthalenic derivatives as new selective MT<sub>2</sub> melatoninerbic ligands. Part II. *Bioorg. Med. Chem.* **2009**, *17*, 2963-2974.
- (62) Shida, C. S.; Castrucci, A. M. L.; Lamy-Freund, M. T. High melatonin solubility in aqueous medium. *J. Pineal Res.* **1994**, *16*, 198-201.
- (63) Csuk, R.; von Scholz, Y. Synthesis of racemic carbocyclic cyclopropanoid nucleoside analogues. *Tetrahedron* **1995**, *51*, 7193-7206.
- (64) O'Neil, M. J., The Merck Index - An Encyclopedia of Chemicals, Drugs, and Biologicals (14th Edition - Version 14.9). Merck Sharp & Dohme Corp., a subsidiary of Merck & Co., Inc.: 2012.
- (65) Glennon, R. A.; Titeler, M.; McKenney, J. D. Evidence for 5-HT<sub>2</sub> involvement in the mechanism of action of hallucinogenic agents. *Life Sci.* **1984**, *35*, 2505-2511.
- (66) Nonaka, R.; Nagai, F.; Ogata, A.; Satoh, K. In vitro screening of psychoactive drugs by [(35)S]GTPgammaS binding in rat brain membranes. *Biol. Pharm. Bull.* **2007**, *30*, 2328-2333.
- (67) Cagnacci, A.; Krauchi, K.; Wirz-Justice, A.; Volpe, A. Homeostatic versus circadian effects of melatonin on core body temperature in humans. *J. Biol. Rhythms* **1997**, *12*, 509-517.
- (68) Glennon, R. A.; Dukat, M.; Grella, B.; Hong, S.; Costantino, L.; Teitler, M.; Smith, C.; Egan, C.; Davis, K.; Mattson, M. V. Binding of beta-carbolines and related agents at serotonin (5-HT<sub>2</sub> and 5-HT<sub>1A</sub>), dopamine (D<sub>2</sub>) and benzodiazepine receptors. *Drug Alcohol Depend.* **2000**, *60*, 121-132.
- (69) Lange, C.; Mix, E.; Frahm, J.; Glass, A.; Müller, J.; Schmitt, O.; Schmöle, A.-C.; Klemm, K.; Ortinau, S.; Hübner, R.; Frech, M. J.; Wree, A.; Rolfs, A. Small

molecule GSK-3 inhibitors increase neurogenesis of human neural progenitor cells.

*Neurosci. Lett.* **2011**, 488, 36-40.

(70) Jiang, W.; Zhang, Y.; Xiao, L.; Van Cleemput, J.; Ji, S.-P.; Bai, G.; Zhang, X.

Cannabinoids promote embryonic and adult hippocampus neurogenesis and produce anxiolytic- and antidepressant-like effects. *J. Clin. Invest.* **2005**, 115, 3104-3116.

(71) Banasr, M.; Hery, M.; Printemps, R.; Daszuta, A. Serotonin-induced increases in adult cell proliferation and neurogenesis are mediated through different and common 5-HT receptor subtypes in the dentate gyrus and the subventricular zone.

*Neuropsychopharmacology* **2004**, 29, 450-460.

(72) Benninghoff, J.; van der Ven, A.; Schloesser, R. J.; Moessner, R.; Moller, H. J.; Rujescu, D. The complex role of the serotonin transporter in adult neurogenesis and neuroplasticity. A critical review. *World J. Biol. Psychiatry* **2012**, 13, 240-247.

(73) Yu, S.; Levi, L.; Siegel, R.; Noy, N. Retinoic acid induces neurogenesis by activating both retinoic acid receptors (RARs) and peroxisome proliferator-activated receptor  $\beta/\delta$  (PPAR $\beta/\delta$ ). *J. Biol. Chem.* **2012**, 287, 42195-42205.

(74) Hardeland, R. Melatonin: signaling mechanisms of a pleiotropic agent. *Biofactors* **2009**, 35, 183-192.

(75) Masana, M. I.; Dubocovich, M. L. Melatonin receptor signaling: finding the path through the dark. *Sci. STKE* **2001**, pe39.

(76) Musshoff, U.; Riewenherm, D.; Berger, E.; Fauteck, J.-D.; Speckmann, E.-J. Melatonin receptors in rat hippocampus: molecular and functional investigations. *Hippocampus* **2002**, 12, 165-173.

(77) Ferguson, F. M.; Fedorov, O.; Chaikuad, A.; Philpott, M.; Muniz, J. R. C.; Felletar, I.; von Delft, F.; Heightman, T.; Knapp, S.; Abell, C.; Ciulli, A. Targeting low-

druggability bromodomains: Fragment based screening and inhibitor design against the BAZ2B bromodomain. *J. Med. Chem.* **2013**, *56*, 10183-10187.

(78) The effect of compounds **16** and **19** on impedance (MT<sub>1</sub>) and cAMP levels (MT<sub>2</sub>) was measured and compared to that of melatonin in Chinese Hamster Ovary cells expressing human recombinant MT receptors by cellular dielectric spectroscopy for MT<sub>1</sub> and in a homogeneous time resolved fluorescent assay for MT<sub>2</sub> by CEREP. The corresponding protocols can be found in the company website: [www.cerep.fr](http://www.cerep.fr).

(79) Urban, J. D.; Clarke, W. P.; von Zastrow, M.; Nichols, D. E.; Kobilka, B.; Weinstein, H.; Javitch, J. A.; Roth, B. L.; Christopoulos, A.; Sexton, P. M.; Miller, K. J.; Spedding, M.; Mailman, R. B. Functional selectivity and classical concepts of quantitative pharmacology. *J. Pharmacol. Exp. Ther.* **2007**, *320*, 1-13.

(80) Rodríguez-Franco, M. I.; de la Fuente Revenga, M.; Pérez, C.; Pérez-Castillo, A.; Morales-García, J. A.; Alonso-Gil, S. Neurogenic compounds comprising melatonin and the efficacy thereof in *in vivo* experiments for use in the treatment of diseases of the nervous system. WO 2014154925 A1, 2014.

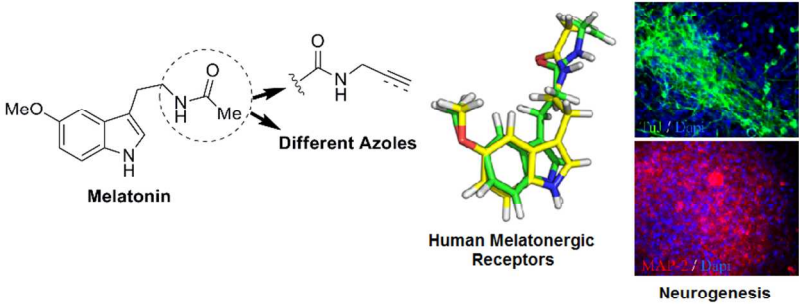
(81) Neuville, P.; Schann, S. Melatonin derivatives and their use for treating neurological dysfunctions. WO 2004085392 A1, 2004.

(82) Boularot, A.; Giglione, C.; Petit, S.; Duroc, Y.; Alves de Sousa, R.; Larue, V.; Cresteil, T.; Dardel, F.; Artaud, I.; Meinnel, T. Discovery and refinement of a new structural class of potent peptide deformylase inhibitors. *J. Med. Chem.* **2007**, *50*, 10-20.

(83) Rensen, M. Cyclisation of 1-Methyl-5-methoxyindole-3-propionic Acid. *Bull. Soc. Chim. Belges* **1959**, *68*, 258-269.

(84) Piotrowska, H.; Serafin, B.; Wejroch-Matacz, K. New amidine derivatives of indole. *Pol. J. Pharmacol. Pharm.* **1975**, *27*, 297-303.

- (85) Audinot, V.; Mailliet, F.; Lahaye-Brasseur, C.; Bonnaud, A.; Le Gall, A.; Amossé, C.; Dromaint, S.; Rodriguez, M.; Nagel, N.; Galizzi, J. P.; Malpoux, B.; Guillaumet, G.; Lesieur, D.; Lefoulon, F.; Renard, P.; Delagrangé, P.; Boutin, J. A. New selective ligands of human cloned melatonin MT<sub>1</sub> and MT<sub>2</sub> receptors. *Naunyn-Schmiedeberg's Arch. Pharmacol.* **2003**, 367, 553-561.
- (86) Fukatsu, K.; Uchikawa, O.; Kawada, M.; Yamano, T.; Yamashita, M.; Kato, K.; Hirai, K.; Hinuma, S.; Miyamoto, M.; Ohkawa, S. Synthesis of a Novel Series of Benzocycloalkene Derivatives as Melatonin Receptor Agonists. *J. Med. Chem.* **2002**, 45, 4212-4221.
- (87) Jorgensen, W. L.; Maxwell, D. S.; Tirado-Rives, J. Development and testing of the OPLS all-atom force field on conformational energetics and properties of organic liquids. *J. Am. Chem. Soc.* **1996**, 118, 11225–11236.
- (88) Morales-García, J. A.; Luna-Medina, R.; Alonso-Gil, S.; Sanz-Sancristóbal, M.; Palomo, V.; Gil, C.; Santos, A.; Martínez, A.; Pérez-Castillo, A. Glycogen synthase kinase 3 inhibition promotes adult hippocampal neurogenesis *in vitro* and *in vivo*. *ACS Chem. Neurosci.* **2012**, 3, 963-971.



TOC graphic  
304x171mm (96 x 96 DPI)



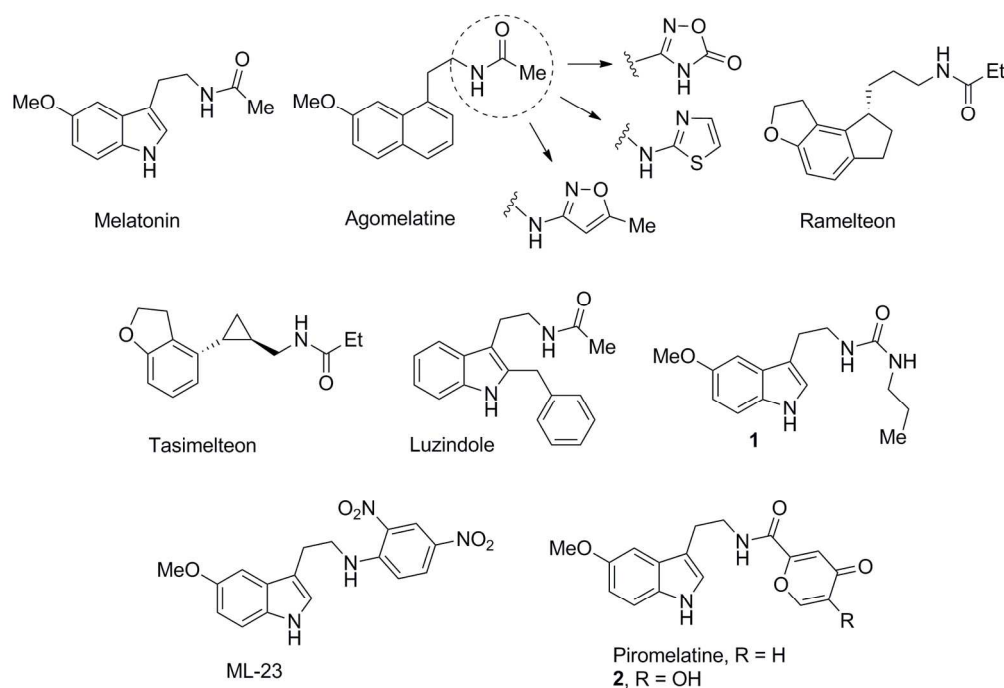


Figure 1. Melatonergic drugs on the market and other selected melatonergic ligands.  
167x114mm (300 x 300 DPI)

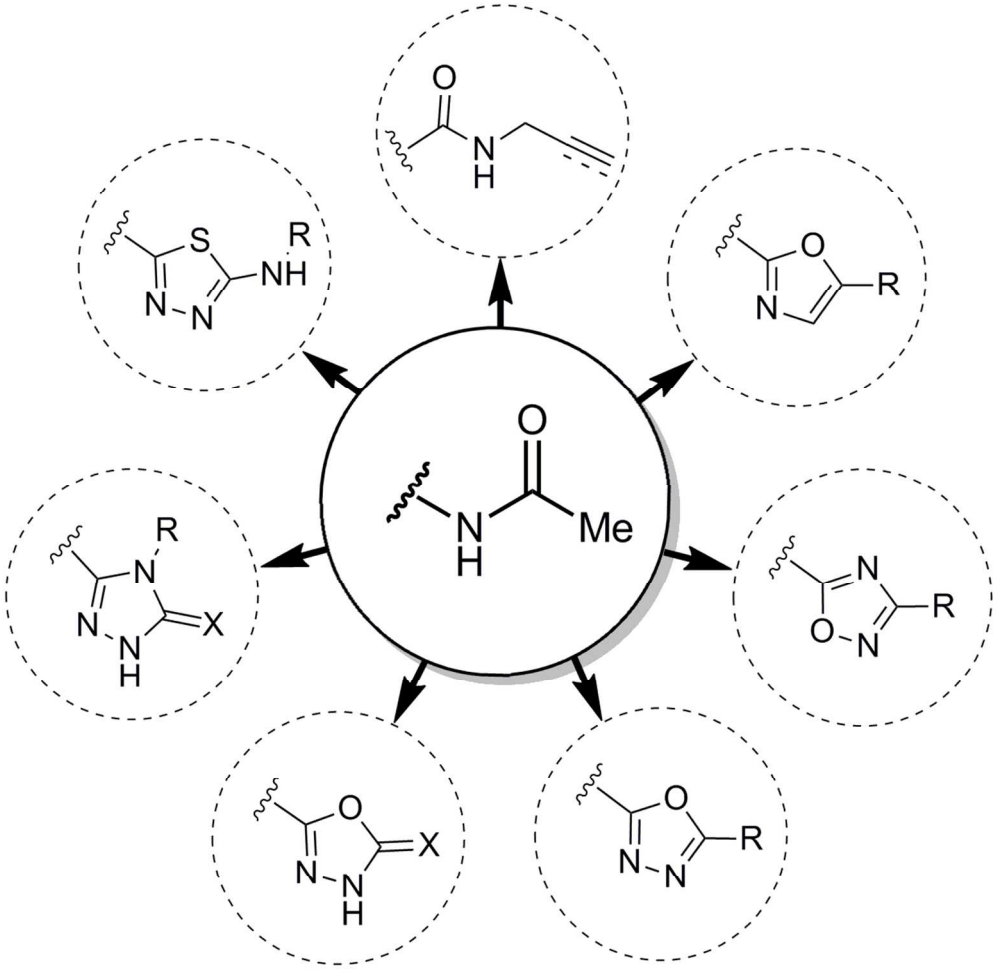


Figure 2. Illustration showing the replacement of the acetamido moiety of melatonin carried out in this work.  
105x102mm (300 x 300 DPI)

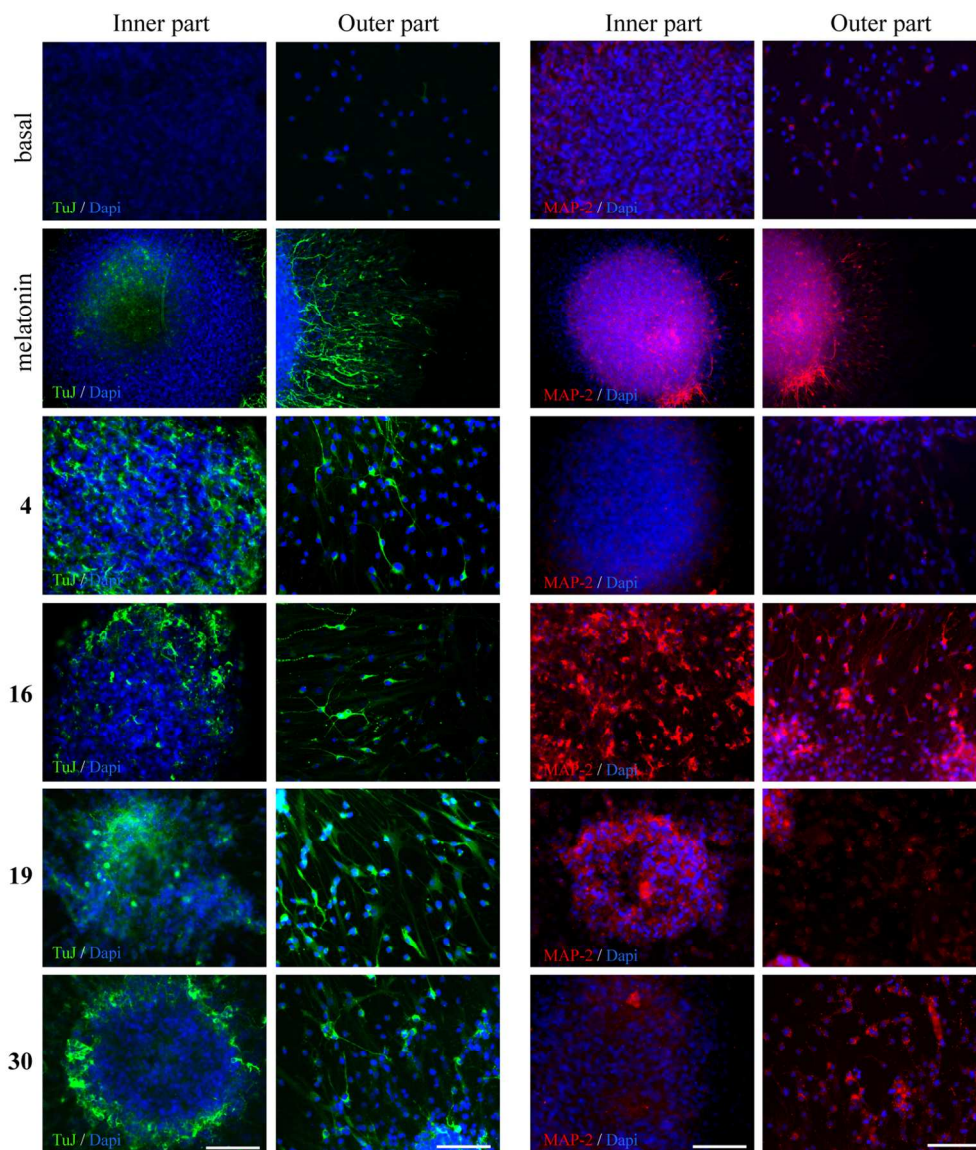


Figure 3. Expression of TuJ1 (green) and MAP-2 (red) in cultured SGZ-derived neurospheres in the presence of different compounds at 10  $\mu$ M. DAPI (blue) was used as a nuclear marker. Scale bar, 200  $\mu$ m. 128x147mm (300 x 300 DPI)

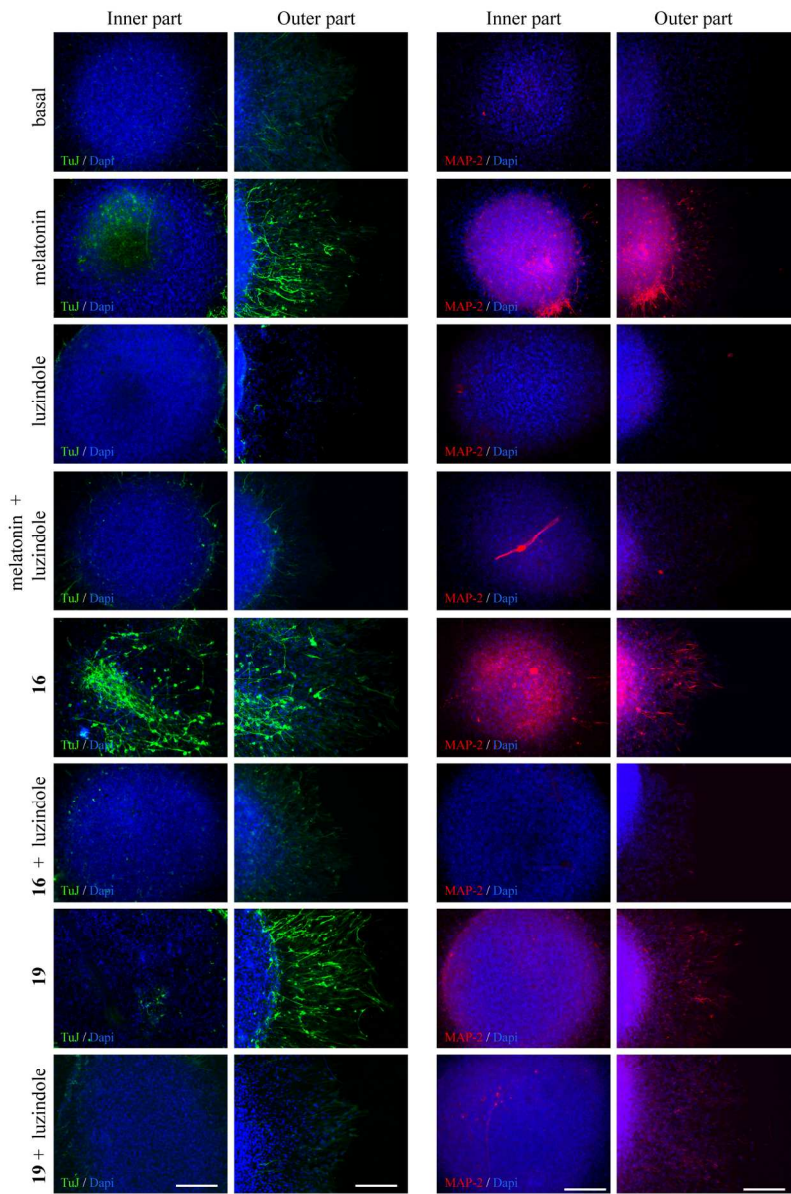


Figure 4. Effect of luzindole (10  $\mu$ M) on the expression of TuJ1 (green) and MAP-2 (red) promoted by melatonin, 16, and 19 at 10  $\mu$ M in SGZ-derived neurospheres. DAPI (blue) was used as a nuclear marker. Scale bar, 200  $\mu$ m. 130x198mm (300 x 300 DPI)



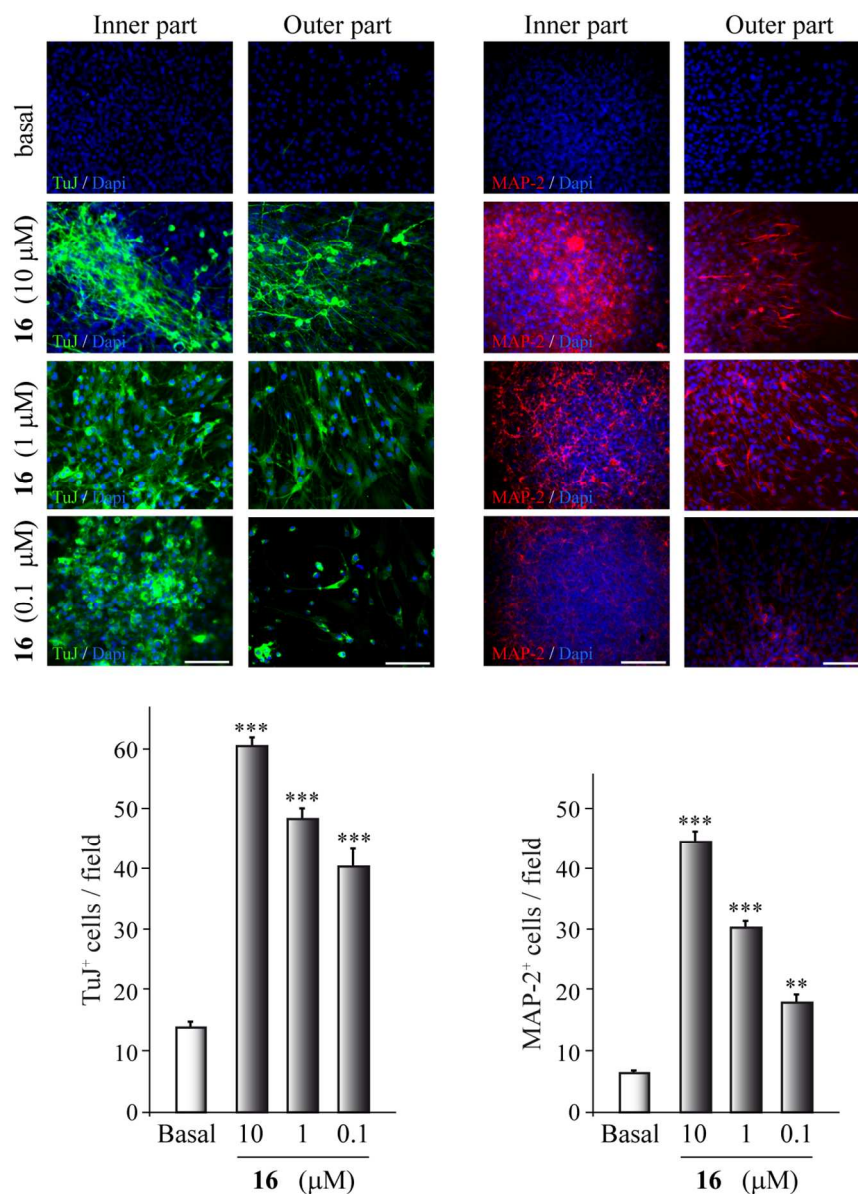


Figure 5. (Top) Dose-response ( $\mu\text{M}$ ) effect of compound 16 on the expression of TuJ1 (green) and MAP-2 (red) in SGZ-derived neurospheres. DAPI (blue) was used as a nuclear marker. Scale bar, 200 $\mu\text{m}$ . (Bottom) Number of TuJ1<sup>+</sup> and MAP-2<sup>+</sup> expressing cells in neurospheres is shown and expressed as the mean  $\pm$  SD.

\*\*  $p \leq 0.01$ ; \*\*\*  $p \leq 0.001$ .  
106x143mm (300 x 300 DPI)

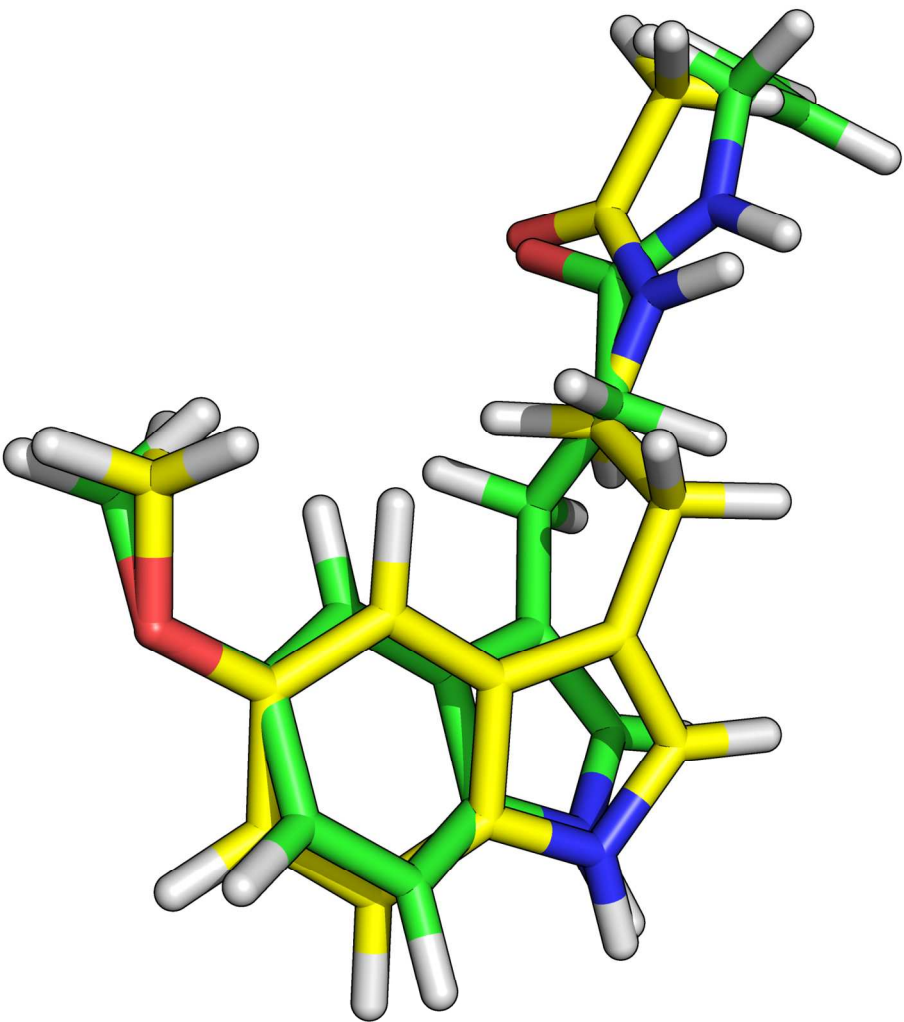


Figure 6. Superposition of melatonin (yellow carbons) in its putative bioactive conformation6 and 6 (green carbons).  
423x529mm (96 x 96 DPI)

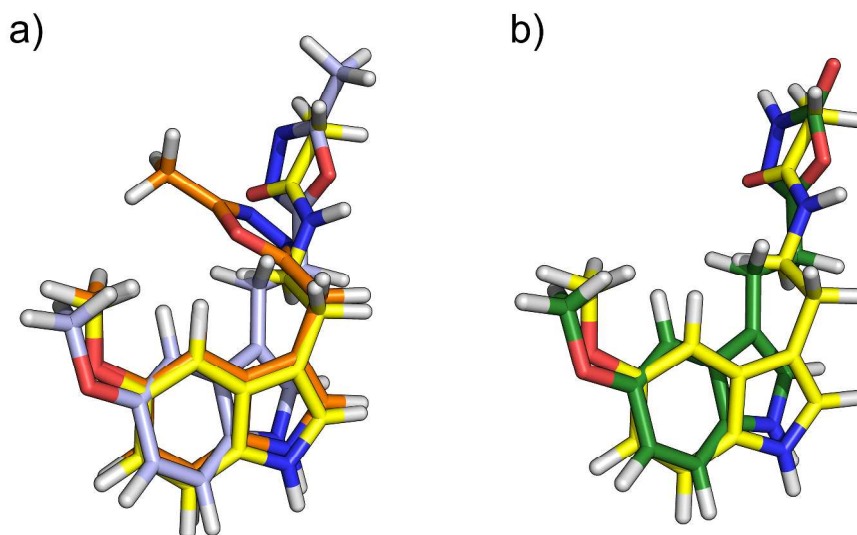


Figure 7. Compounds 15 (orange carbons), 16 (gray carbons) (panel a) and compound 19 (green carbons) (panel b) superposed on melatonin (yellow carbons).  
1005x550mm (96 x 96 DPI)

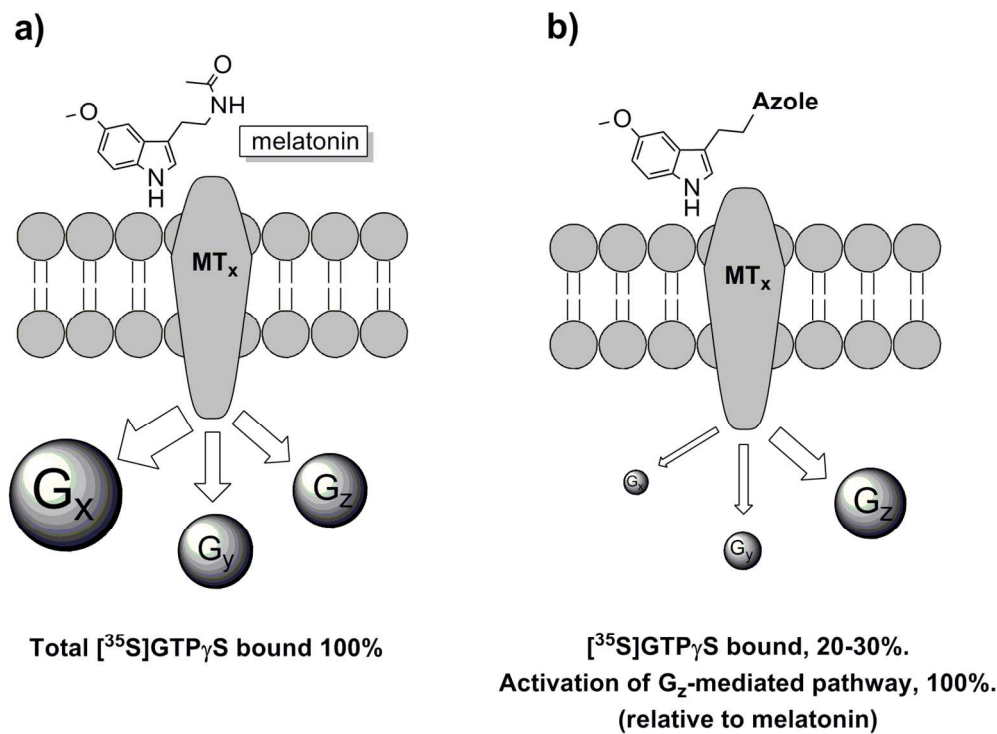
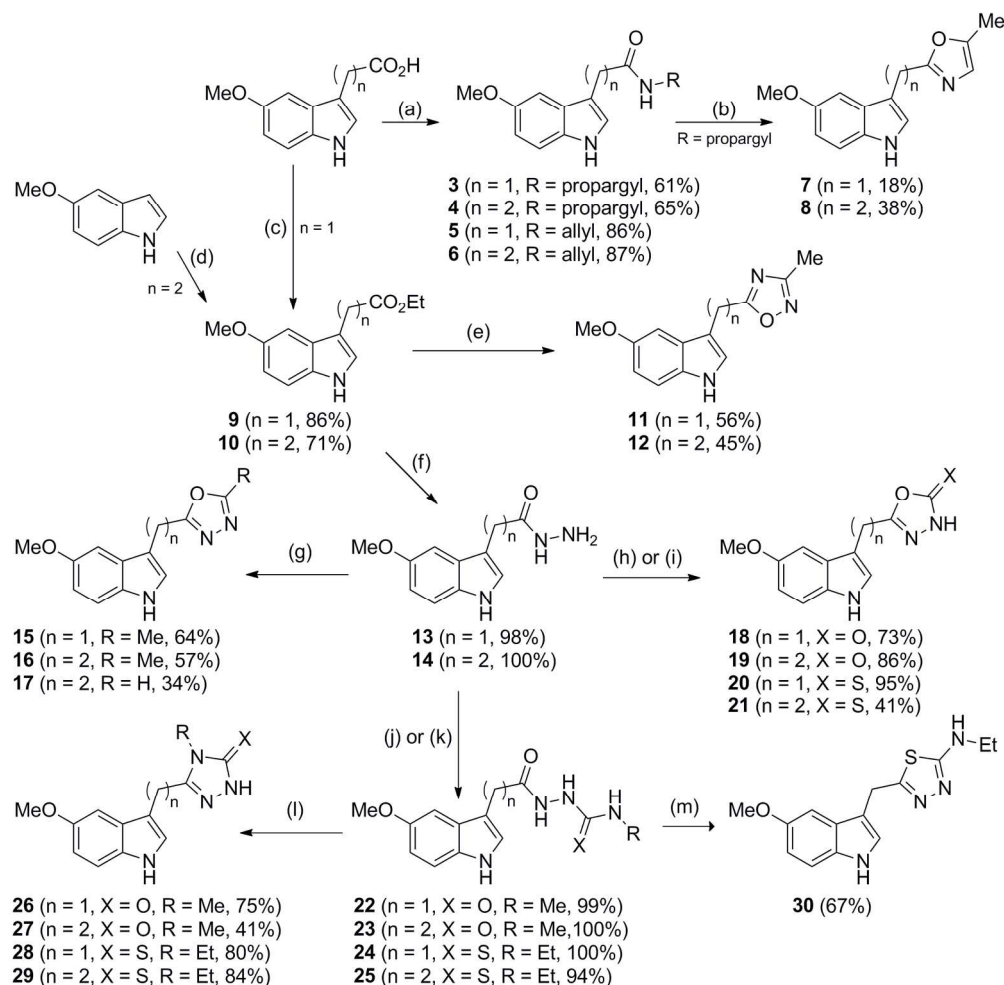


Figure 8. Schematic representation of the functional selectivity hypothesis of melatonin-azole derivatives at MT receptors. (Panel a) Melatonin, the reference and native ligand, binds to melatonergic receptors coupled to G-proteins, that upon activation bind [<sup>35</sup>S]GTP<sub>γ</sub>S. The amount of G-protein activated is taken arbitrarily as 100%. The size and names of the G-proteins are fictional and represent the relative population of certain activated G-protein isoforms. (Panel b) The low binding of [<sup>35</sup>S]GTP<sub>γ</sub>S upon binding of melatonin-azole derivatives to melatonergic receptors could indicate the preferential activation of certain populations of MTn-Gn, and subsequently, of their corresponding signaling pathways.

140x103mm (300 x 300 DPI)





Scheme 1. Reagents and conditions: (a) CDI, CH<sub>2</sub>Cl<sub>2</sub>, propargylamine or allylamine, rt; (b) AuCl<sub>3</sub>, CH<sub>2</sub>Cl<sub>2</sub>, N<sub>2</sub>, rt; (c) H<sub>2</sub>SO<sub>4</sub> (cat.), EtOH, reflux; (d) ethylacrylate, ZrCl<sub>4</sub> (anh.), CH<sub>2</sub>Cl<sub>2</sub>, N<sub>2</sub>, rt; (e) acetamidoxime, NaH, THF, mol. sieves, 80 °C; (f) hydrazine hydrate, 150 °C (mw), 45 min; (g) orthoester, AcOH (cat.), 125 °C (mw), 1 h; (h) compounds with X = O: CDI, TEA, THF, 100 °C (mw), 10 min; (i) compounds with X = S: CS<sub>2</sub>, EtOH, KOH (aq.), 150 °C (mw), 10 min; (j) intermediates with X = O and R = Me: MeNCO, EtOH, rt; (k) intermediates with X = S and R = Et: EtSCN, EtOH, rt; (l) NaOH (aq.), EtOH, 100 °C (mw), 15 min; (m) POCI<sub>3</sub>, rt.

170x167mm (300 x 300 DPI)